Moth-Inspired Chemical Plume Tracing on an Autonomous Underwater Vehicle

Wei Li, Jay A. Farrell, Shuo Pang, Richard M Arrieta

Abstract—This paper presents a behavior-based Adaptive Mission Planner (AMP) to trace a chemical plume to its source and reliably declare the source location. The proposed AMP is implemented on a REMUS Autonomous Underwater Vehicle (AUV) equipped with multiple types of sensors measuring: chemical concentration, the flow velocity vector, and AUV position, depth, altitude, attitude and speed. This article describes the methods and results from experiments conducted in November 2002 at San Clemente Island, California using a plume of Rhodamine dye developed in a turbulent fluid flow (i.e., near shore ocean conditions). These experiments demonstrated chemical plume tracing over 100 meters and source declaration accuracy relative to the nominal source location on the order of tens of meters.

The designed maneuvers are divided into four behavior types: finding a plume, tracing the plume, reacquiring the plume, and declaring the source location. The tracing and reacquiring behaviors are inspired by male moths flying upwind along a pheromone plume to locate a sexually receptive female. All behaviors are formulated by perception and action modules and translated into chemical plume tracing algorithms suitable for implementation on a REMUS AUV. To coordinate the different behaviors, the subsumption architecture is adopted to define and arbitrate the behavior priorities. AUVs capable of such feats would have applicability in searching for environmentally interesting phenomena, unexploded ordnance, undersea wreckage, and sources of hazardous chemicals or pollutants.

Index Terms—Autonomous vehicles, behavior-based planning, subsumption architecture, chemical plume tracing.

I. INTRODUCTION

A potential application for robotics research is an Autonomous Underwater Vehicle (AUV) to search for environmentally interesting phenomena, unexploded ordnance, undersea wreckage, and sources of hazardous chemicals or pollutants. A key issue in designing such an AUV system is development of an Adaptive Mission Planner (AMP) that is able to navigate the vehicle in response to real-time sensor information to find the plume, trace the plume towards its source, and declare the source location. In this article, this problem will be referred to as Chemical Plume Tracing (CPT).

Olfactory-based mechanisms have been hypothesized for a variety of biological behaviors [1], [2], [3]: homing by Pacific salmon [4], foraging by Antarctic procellariiform seabirds [5], foraging by lobsters [6], [7], foraging by blue crabs [8], and mate-seeking and foraging by insects [9], [10], [11]. Typically, olfactory-based mechanisms proposed for biological entities combine a large-scale orientation behavior based in part on olfaction with a multisensor local search in the vicinity of the source. Long-range search is documented in Antarctic procellariiform seabirds, possibly by olfactory landmark navigation, over 1000 km [5]. Plume tracing by moths at ranges of 100-1000 m is described on p. 276 in [10]: "Rau and Rau (1929) provided perhaps the most extensively documented case of long-distance mate finding by luring male silkworm moths released several kilometers from caged virgin females held on a second-story roof of their home in St. Lous, Missouri [12]. C.H. Fernald also demonstrated evident location of distant females in the gypsy moth (*Lymantria dispar*) in New England: a few males released several kilometers away located females after several hours (Forbush and Fernald 1896)." Unfortunately, recapture of released males "cannot disentangle the contributions of ranging flight which might bring a male into contact with a pheromone plume and of pheromone-dictated maneuvers which close contact between pheromone sender and receiver" [10].

Factors that complicate CPT include the chemical source concentration being unknown, the advection distance of any detected chemical being unknown, and the flow variation with both location and time. Both engineered [13] and biomimetic [14], [15], [16], [17], [18], [19] strategies have been evaluated in simulation. Such strategies attempted to solve the CPT problem based on fluid flow and instantaneous chemical concentration measurements acquired only at the vehicle location. Belanger and Willis [15], [16] presented plume tracing strategies, including counter-turning strategies, intended to mimic moth behavior and analyzed the performance in a computer simulation. Grasso et al. [14], [17], [18] evaluated biomimetic strategies and challenged theoretical assumptions of the strategies by implementing biomimetic strategies on their robot lobster. Robots that attempt plume tracing in laboratory environments are also described in [20], [21], [22], [23]. The work in [24], [25], [26], [27] tested some hypothesized insect behaviors for plume tracing by using mobile robots in labora-

tories. For example in [24], Grasso and Atema compared the plume tracing performance of three plume tracing strategy variations by using a single-sensor or two sensors detecting fluorescence. Li et al. [19] developed, optimized, and evaluated counter-turning strategies inspired by moth behavior. Of the above work, none discussed the issue of source declaration and only [13] and [19] discuss scales significantly larger than a few meters. Whereas experimental studies described in the existing literature have occurred in structured laboratory environments, only those presented herein and in [28] and [29] occurred in a complex fluid environment such as the near shore ocean with length-scales over 100 meters.

Fundamental aspects of these research efforts include sensing the chemical, sensing or estimating the fluid velocity, and generating a sequence of searcher speed and heading commands such that the resulting AUV motion is likely to approach the chemical source. In each of the articles of the previous paragraph, the algorithms for generating speed and heading commands used only instantaneous (or very recent) sensor information. Typical orientation maneuvers include: sprinting upwind upon detection; moving crosswind when not detecting; and, manipulating the relative orientation of a multiple sensor array, either to follow an estimated plume edge or to maintain the maximum mean reading near the central sensor.

An initial approach to designing an AUV plume-tracing strategy might attempt to calculate a concentration gradient, with subsequent plume tracing based on gradient following. At medium and high Reynolds numbers, the evolution of the chemical distribution in the flow is turbulence dominated [3], [30], [31]. The result of the turbulent diffusion process is a highly discontinuous and intermittent distribution of the chemical [9], [30], [31], [32], [33], [34], [35]. A dense array of sensors distributed over the area of interest and a long time-average of the output of each sensor (i.e., several minutes per sensor) would be required to estimate a smooth (time-averaged) chemical distribution. However, the required dense spatial sampling and long time-averaging makes such an approach ineffective for implementation on an AUV. In addition, even decameters from the chemical source in the direction of the flow the gradient is too shallow to detect in a time-averaged plume. For an 'instantaneous' plume, the gradient is time-varying, steep, frequently in the wrong direction, and its evaluation would require numerous sensors. The essential issue that results in gradient algorithms being ineffective for a single AUV in a turbulent flow environment is that the AUV sampling is too coarse relative to the spatial and temporal rates of change that can occur in the environment.

This paper systematically presents a novel approach to design and implement a complete AMP strategy, including source declaration. The strategy uses a subsumption architecture with certain behaviors motivated by the maneuvering behaviors of moths flying upwind along a pheromone plume. The first step in designing the AMP strategy is to implement behaviors for finding the plume, tracing the plume towards its source, and maneuvering to accurately declare the source location. The second step is to coordinate the different behaviors using the subsumption architecture. The proposed CPT strategy is different from the ones in [14]-[27] in a variety of ways. First, this paper uses a subsumption architecture to co-ordinate the AMP behaviors. Second, our Maintain-Plume behavior is decomposed into Track-In plume and Track-Out plume activities, which have each been studied and optimized by Monte Carlo methods [19]. Third, we introduce a Reacquire-Plume behavior that is modeled on the idea of moth 'casting' (discussed further in the last paragraph of Section II), but designed to be feasible for implementation by an AUV. Fourth, the CPT strategy is completed by design and integration of a Declare-Source method. The in-water results reported herein are the first to take CPT from the lab to a complex real environment. While the results demonstrate efficient plume tracing they also show that the efficiency of the Declare-Source behavior is difficult to achieve and critical to mission performance. For biological entities (e.g., moths), the conclusion of plume tracing may not be based on olfaction alone, but could be aided by vision, sight, auditory, and/or tactile cues. The mechanical structure of the REMUS AUV differs from the structure of the laboratory robots (and also most biological entities) that were the focus of previous experimental studies. Most laboratory robots drive their wheels differentially to control heading. Therefore, they can change their orientation with a near zero turning radius. In contrast, the REMUS vehicle is fin controlled. Therefore, it requires a large (5-10 m) turning radius to change orientation. This maneuvering limitation had to be addressed in the strategy design. Finally, source declaration on an AUV must address practical issues such as the time-varying position estimation error. The experiments described in this article utilize a new source declaration algorithm that worked reliably, but was relatively slow. This article presents a complete CPT strategy; a thorough analysis of successful, large-scale, in-water experimental data acquired at San Clemente Island in November 2002; and, suggestions for future improvements.

The assumptions made herein relative to the chemical and flow are that the chemical is a neutrally buoyant and passive scalar advected by a turbulent flow. The REMUS AUV is capable of sensing position, chemical concentration, and flow velocity. In the proposed strategy, the concentration sensor works as a "binary detector." The binary detector provides at 9 Hz a Boolean value indicating the presence of chemical. The Boolean value is '1' if the chemical concentration is above the threshold; while the Boolean value is '0' if the chemical concentration is below the threshold. Boolean sensing is also used in e.g., [13], [15], [16], [19], [23]. Boolean sensing combined with differential sensing across two antennae is considered in [17]. The strategy presented herein is implemented to solve the plume-tracing problem in two dimensions. A main motivation for implementing the algorithms in two dimensions is the computational simplification achieved; however, neutral buoyancy of the chemical [36] or stratification of the flow [37] will often result in a plume of limited vertical extent, which may be approximated as a two-dimensional problem. To take advantage of these features, the AUV will operate in a fixed-altitude terrain-following mode intended to keep the vehicle in the bottom boundary layer.

This paper is organized as follows. In Section II, we discuss various aspects of the CPT mission. In Section III, we present the subsumption architecture for the Adaptive Mission Planner. In Section IV, we formulate the behaviors and translate them into algorithms. In Section V, we analyze the results

from in-water experiments conducted at San Clemente Island in November 2002. In Section VI, we draw some conclusions about the AMP strategy and experimental results.

II. MISSION PROFILE

The goal of the CPT AUV is to locate the source of a chemical that is transported in a turbulent fluid flow. We assume that the AUV is constrained to maneuver within a rectangular region referred to as the operation area (OpArea) that is specified by the test director prior to the start of the mission. The OpArea is defined by the geodetic latitude and longitude coordinates of the corners of the rectangle. Latitude and longitude are also used for reporting important locations. Specific information about the experimental OpArea is given in Section V. In addition to geodetic coordinates, the AMP maintains two other sets of coordinates for convenience of planning and data presentation. The North-East (N, E) coordinate system has axes aligned with latitude and longitude, respectively, but with coordinates measured in meters and the origin of the coordinate system at the center of the OpArea. The planning space coordinates are denoted (x, y). The x-axis is aligned with the long axis of the rectangular OpArea. When drawn in the plane of the page, as in Figs. 1 and 3, the x-axis is drawn positive to the right. The y-axis is drawn as positive downward. The (N, E) coordinates are related to the (x, y) coordinates through a simple rotation about the local vertical axis. The heading θ is defined positive in the clockwise direction. Typically, the OpArea is defined with its longer axes approximately parallel to the shoreline. Also, the flow is typically dominant in the direction parallel to the shoreline. Therefore, in planning space coordinates the direction of the (mean) flow will often be within 45 degrees of the x-axis. This information is not used by the planner, but is convenient for data presentation.

Fig. 1 shows a hypothetical plume tracing trajectory in the planning coordinate system. The trajectory indicates two mission components labeled as Mission A and Mission B. Mission A is a preplanned (off-line) trajectory controlled by the original mission planner developed by Woods Hole Oceanographic Institute (WHOI). Fig. 1 shows the entire Mission A as a light dashed line; however, the AUV only performs the portion that is indicated by the wide solid line. Mission B is implemented and managed on-line by the AMP to achieve plume tracing and chemical source declaration by reacting in real-time to chemical detection and flow information. In our experiments, Mission A will be used to drive REMUS to a desired starting point in the OpArea. At that location, Mission B activates, performs its CPT tasks and then deactives to allow Mission A to drive the AUV to a rendezvous location for pickup. For vehicle security, Mission A would also take over if the AUV moved sufficiently far (i.e., 30m) outside the specified OpArea. This did not occur in the set of experiments described herein.

During Mission B, the AUV will search for a specific chemical within the OpArea. If the chemical is detected, the vehicle should trace the chemical plume to its source and accurately declare the source location. For plume tracing tasks, the location of pheromone-emitting females by flying male moths is considered a remarkable case of chemical-guided

navigation. The AMP strategy described herein is inspired by biological behaviors hypothesized from observations of moths [9], [10], [11], [15], [16]. These hypothesized behaviors can be summarized as follows. When a moth detects pheromone, it tries to maintain contact with the plume and to move upwind towards the source location. The maneuver is exhibited as a short sprint predominantly in the upwind direction. Repeated pheromone encounters result in the moth progressively approaching the chemical source. When a moth has not detected pheromone for a sufficiently long period of time, it ceases upwind movement and performs progressively widening crosswind excursions, termed 'casting.' In this case, the moth appears to be searching for pheromone near the position where it was last detected. This reacquiring behavior can continue for several seconds until either chemical is again detected or the moth behavior changes. If the moth fails to detect pheromone again, it may return to the Finding-Plume behavior used initially for location of the plume. The moth approach to finding the plume has been studied in the field e.g. [11], [38], but still is not well understood due to difficulties related to tracking the moths over long distances and to knowing when an in-flight moth is detecting pheromone.

III. SUBSUMPTION ARCHITECTURE

Our approach uses a behavioral control approach [39]-[45], with the behaviors being coordinated in a subsumption architecture [41]. For CPT we use four behaviors: Find-Plume, Maintain-Plume, Reacquire-Plume, and Declare-Source. In this set of behaviors, Maintain-Plume and Reacquire-Plume are moth inspired. The Find-Plume and Declare-Source behaviors are engineering-based. The CPT AMP subsumption architecture is shown in Fig. 2. The control commands from the planner to the vehicle guidance and control functions are speed and heading commands. The inhibition approach is used to arbitrate between the commands from the various behaviors to determine the commanded output of the AMP. In Fig. 2, the circles labeled with an 'S' are subsumption modules. The output of the subsumption module is connected to the top input of another subsumption module. If the top input to the subsumption module has any value, then the output of the subsumption module assumes that value; otherwise the output of the subsumption module takes the value of its left input. The following text discusses the priorites imposed by the subsumption architecture in Fig. 2 with brief descriptions of the behaviors. A detailed description of each behavior in Fig. 2 is provided in Section IV.

For the AMP CPT strategy, the Declare-Source behavior has the highest priority. Once that behavior has declared the source location, it defines its commanded outputs to drive the vehicle to a home location. The Declare-source output commands block the commands from any other behaviors. The Maintain-Plume behavior includes Track-In and Track-Out activities. Track-In tries to make rapid progress toward the source while chemical is being detected. Track-Out manipulates the AUV heading relative to upflow in the time immediately following the loss of chemical detection to try to rapidly recontact the plume. These activities have the second and third highest priorities. For these activities to be controlling the vehicle, the AUV will either be detecting or have recently

been detecting an above threshold concentration of chemical. To ensure that maneuvers to maintain contact with the plume occur in an uninterrupted fashion, Maintain-Plume behaviors block the commands from any other behaviors except for those following source declaration.

The Move-To-Field behavior has the lowest priority. This behavior is only used to send the vehicle to a desired location in the OpArea at the beginning of the mission. The output commands from this behavior are blocked once the vehicle activates any other behaviors. The Find-Plume behavior issues commands designed to explore the entire OpArea. The resulting trajectories are similar to a ball bouncing on a billiard table. The Find-Plume behavior will continue until either a timeout condition is achieved or a chemical detection event causes another behavior to become active. The priority of the Reacquire-Plume behavior is above that of the Find-Plume behavior. If the Track-Out activity fails to detect chemical within a given time period, then the Maintain-Plume behavior deactivates. In this case, the Reacquire-Plume behavior will maneuver the AUV in the vicinity of the most recent chemical detection location. This is similar to moth casting. The hope is that the local area search directed by the Reacquire-Plume behavior will recontact the plume. If it does not, then its deactivation causes the Find-Plume behavior to take over. The Find-Plume behavior may be time consuming since it will potentially search the entire OpArea to detect chemical.

IV. FORMULATION OF BEHAVIORS

The next important step is to design an algorithm that will generate a feasible AUV trajectory to reliably achieve the goal of each behavior. Based on schema theory [42], the behaviors of the REMUS vehicle are decomposed into perception and action modules. Schema theory is well suited for transferring theoretical concepts into the object-oriented programming constructs used to implement the behaviors.

The perception module is identical for all behaviors. The REMUS computer sends messages containing the sampled chemical concentration σ and vehicle state to the AMP at 9 Hz and acoustic Doppler data at 0.5 Hz. The planning cycle for generating the heading and speed commands is 1 Hz. For the AMP planning cycle, the perception module calculates the maximum value from the nine most recent chemical concentration samples and uses the most recent vehicle state. The perception module processes the vehicle velocity and acoustic Doppler data to estimate the flow velocity of the fluid relative to the earth. Since this estimated flow velocity is very noisy, the flow used by the AMP is averaged over 100 sec. The outputs from each of the action modules are the commands for the vehicle speed v and heading θ. Prior to each run, the speed command is set, as a constant value, by the test director. The tradeoffs related to the choice of the commanded speed are that increasing the speed searches the region faster, but also results in fewer concentration measurements per meter traveled since the sample rate is fixed.

A. Find-Plume Behavior

The problem of determining the optimal direction to search for a chemical plume in a time-varying flow is addressed theoretically in [46], [47]. When the flow is slowly time-varying relative to the rate that the searcher can explore, those results show that cross-flow search provides more information than along flow search. Since the mission time can be scheduled and a slowly time-varying flow generates a well-defined plume that facilitates plume tracing, the mission times are selected during periods when the flow is slowly-time varying. Using these facts, the Find-Plume behavior was designed to dominantly implement a cross-flow search. The behavior also implements a smaller along-flow component to ensure that the entire search region will ultimately be explored.

Definition: The Find-Plume behavior is designed without any assumptions about the location of the source within the OpArea. The behavior does incorporate the fact that when there is a source in the OpArea, the AUV will be more likely to detect chemical along a downflow edge than along an upflow edge. The Find-Plume behavior could initiate in two situations. The first situation is at the start of the mission prior to any chemical being detected. The second situation is after the Track-In, Track-Out, and Reacquire behaviors have each turned off due to a lack of recent chemical detections. The main features of this behavior are: the AUV should move predominantly across the flow; the trajectory should contain an along the flow component to cause the vehicle to explore new territory within the OpArea; and, when the upflow boundary is eventually encountered, the vehicle should rapidly move to the downflow edge of the OpArea. The commanded heading is defined as θ=flow_dir+sign(η)*dθ, which is an offset to the computed flow direction denoted by 'flow_dir.' The sign of the variable η will be either ±1. The variable dθ can only take on one of the two constant values dθ_{up} and dθ_{down}. A typical AUV trajectory is depicted in Fig. 3. A logic flow diagram for the algorithm is shown in Fig. 4 and discussed below.

Each time that the CPT algorithm initiates the Find-Plume behavior, the initial commanded vehicle direction is determined as follows. The initial vehicle position (x_0, y_0) divides the planning space into four sub-areas as illustrated in Fig. 3. With a uniform distribution of probable source locations, the largest sub-area is most likely to contain the source. Therefore, the initial values of the parameters η and dθ are defined so that the AUV will drive into the largest of the four sub-areas. If at any time the sensed concentration σ is above the detection threshold, then Track-In will activate which will inhibit the Find-Plume commands. As long as σ is below threshold, the AUV will continue to maneuver for plume finding.

While the vehicle maneuvers, the Find-plume behavior checks if the AUV is in the OpArea. While in the OpArea, the flow relative offset is constant since η and dθ are constant. When the AUV reaches an OpArea boundary, then either the value of η or dθ will change. If the AUV reaches X_{min} (i.e., the left boundary of planning space), then the down-flow search offset angle dθ_{down} is used. If the AUV system reaches X_{max} (i.e., the right boundary of planning space), then the up-flow search offset angle dθ_{up} is used.

The variable η defined as $\eta = 0.5(Y_{min}+Y_{max})$-y points from the vehicle location toward the x-axis. The value of η is

recomputed only when the AUV leaves the OpArea through either its upper or lower boundaries in planning space (i.e., $y < Y_{min}$ or $y > Y_{max}$). The sign function

$$\text{sign}(\eta) = \begin{cases} 1 & \eta >= 0 \\ -1 & \eta < 0 \end{cases}$$

results in a commanded value of the heading such that the vehicle returns to the OpArea and drives towards the opposite y-boundary of the OpArea.

When the OpArea is large and there is no prior information about the source location (i.e., uninformed search), the Find-Plume behavior may consume a significant amount of time to find the plume. Therefore, once the chemical plume is detected, the other behaviors are designed to maintain at least intermittent contact with the plume, to decrease the likelihood that the AMP returns to the Find-Plume behavior.

Since the OpArea is defined by the test director, the Find-Plume behavior has only two adjustable parameters: $d\theta_{up}$, and $d\theta_{down}$. As a result of Monte Carlo simulation studies described in [19] the up-flow and down-flow search offsets were selected as $d\theta_{up} = 125$ deg and $d\theta_{down} = 60$ deg.

B. Maintain-Plume Behavior: Track-in and Track-out

This section defines the Track-In and Track-Out activities of the Maintain-Plume behavior. This behavior was inspired by those hypothesized for male moths based on experimental observations: when a male moth detects pheromone, it modulates its steering, speed and counter-tuning frequency to maintain intermittent contract with the plume while achieving movement toward the source location. Similarly, once chemical has been detected, the purpose of the Maintain-Plume activities is to keep the AUV *in the plume* while making progress toward its source.

The phrase 'in the plume' requires clarification as different researchers define it differently. Because the plume is composed of filaments of chemical transported by a turbulent fluid flow, it is possible for the sensor to be between filaments without detecting chemical; therefore, the sensed chemical concentration is an intermittent signal. The fluid dynamics literature contains definitions of plume length scales based on the distances over which signals are correlated, see e.g. [48], [49] for a discussion of length scales relative to biological chemical sensing. Such definitions are useful for theoretical discussions, but impractical for behavior design. For this article, we will say that the AUV is "in the plume" at time t if the sensed chemical concentration has been above threshold at least once in the previous λ seconds. The AUV is not 'in the plume' at time t if the sensed chemical concentration has not been above threshold within the last λ seconds. Note that in this definition, the AUV being in the plume at time t does not require the sensed chemical concentration to be above threshold at time t. Note also, that if the AUV has recently detected chemical then it is likely to be in or near the plume. As the time since the last detection increases, then it is increasingly likely that the vehicle is out of the plume.

Definition: To maintain contact with the plume at least intermittently, the Maintain-Plume behavior may use two activities: Track-In and Track-Out. Fig. 5 will be useful to describing these activities. The logic flow diagram for the Maintain-

Plume behavior is shown in Fig. 6. In Fig. 5, the gray patches represent chemical filaments. In relation to Fig. 5, we assume that chemical is detected when the trajectory is within a filament. The sequence of thin solid arrows that are connected head-to-tail indicates the AUV chemical sensor trajectory. The three wider solid arrows indicate the local flow direction at the time the sensor was at the corresponding location. The black dots indicate times at which a behavior change occurs. When the sensed chemical concentration is above threshold, then the Track-In activity becomes active, for example, ΔT_1 and ΔT_3 in Fig. 5. If the sensed chemical is below threshold, but was above threshold within the last λ seconds, then the Track-Out action is active, for example, ΔT_2 and ΔT_4 in Fig. 5. If the AUV does not detect above-threshold concentration during the previous λ seconds, then the Maintain-Plume behavior turns off, which causes the Reacquire behavior to become active, for example at $t = T_{last} + \lambda$ as shown in Fig. 5.

The Monte Carlo simulation analysis described in [19] studied various Maintain-Time strategies and various choices of design parameters for each strategy. The main performance measures were robustness to environmental factors, ability to maintain plume contact, and ability to make progress towards the source. A major result of that study was that counter-turning strategies led to significant increases in performance. Upon losing contact with the plume, such strategies intentionally turn in a direction that is considered most likely to contain the plume. The strategy of Fig. 6 implements one of the counter-turning strategies.

The Maintain-Plume behavior activates when the AUV detects above threshold chemical concentration. The Track-In action activates first. The Track-In activity steers the AUV to move directly up-flow. Near the source, where the plume axis is aligned with the flow, this will result in rapid progress towards the source. Further from the source, where the plume axis and local flow may not align, the AUV is likely to exit the plume prior to reaching the source.

When the sensed concentration drops below threshold, the Track-Out activity adds an offset β from the upflow direction to the commanded heading. The offset β and the commanded heading θ are computed as

$$\varphi = \text{atan2}\big((y_{last} - y), (x_{last} - x)\big)$$
$$\Delta\varphi = \text{flow\_dir} - \varphi$$
$$\beta = 10\,\text{sign}(\Delta\varphi)$$
$$\theta = \text{flow\_dir} + 180 + \beta$$

where (x_{last}, y_{last}) is the last location at which chemical was detected, ϕ defines the direction of the vector from the current AUV location to the last detection point, and $\Delta\phi$ is the error between the flow direction and ϕ. Assuming that the vehicle yaw is currently within 90 deg of upflow (as it should be during Track-In), the sign of $\Delta\phi$ indicates the direction relative to upflow (right = 1 or left = -1) that is more likely to contain the plume. The magnitude of the offset relative to upflow is selected to be 10 deg based on the analysis in [19] and simulations using a relatively accurate vehicle dynamic model. The Track-Out activity continues until either chemical

is again detected or the time since the last detection exceeds λ seconds.

The only two tunable parameters in the Maintain-Plume strategy are λ and the magnitude of β. The effects on performance of changing each parameter were studied in [19]. Based on those studies and issues related to vehicle maneuverability λ was selected as 8.5 seconds.

C. Reacquire-Plume Behavior

Biological studies such as [50], [51] report that male moths cast when they appear to lose contact with the pheromone plume. Casting implies that the moth ceases upwind movement and performs progressively widening crosswind excursions. Such casting behavior results in a local search for the plume in the vicinity of the position where plume contact was lost.

Definition: The objective of the Reacquire-Plume behavior is to reacquire contact with the plume in the situation where chemical has not been detected for at least λ seconds. The behavior was inspired by those hypothesized for moths, but also constrained by vehicle maneuverability issues. When the Reacquire-Plume behavior initiates, chemical has been previously detected approximately λ seconds ago at location (x_{last}, y_{last}). Therefore, similar to moth casting behavior, the Reacquire-Plume behavior will cause the AUV to perform maneuvers across the flow in the vicinity of the location (x_{last}, y_{last}).

There are a few principal reasons that upflow motion within the plume might lead to loss of contact with the plume [52]. First, the internal structure of plumes is patchy, that is, in certain locations the signal is not present or it is below the threshold of detection. Due to this patchiness, the vehicle mounted sensor may pass between chemical filaments without detecting any chemical even though the AUV is in the plume. This is the reason for using a non-zero value of λ. Second, the upflow motion may lead out of the plume since meander of the plume centerline can cause the plume centerline to not be parallel to the local flow direction. Third, when the vehicle approaches the plume source, continued upflow motion will cause it to pass the source. It is important to consider all three of these cases while designing the Reacquire-Plume behavior module.

The cloverleaf trajectory that we selected is illustrated in Fig. 7, where the assumed flow direction is from the left to the right. The center of the cloverleaf maneuver is (x_{last}, y_{last}). The length of each leaf is defined by the parameter d_{leaf}. The minimum value of d_{leaf} is constrained to be larger than the AUV turning radius. Leaves 1 and 2 (upper left and lower left) provide significant crossflow excursions designed to contact the plume in meander situations. Based on the sign of β, the AMP can estimate on which side of the plume the vehicle is located and select the most appropriate of leaves 1 or 2 to execute first. Leaf 3 is aligned with the plume centerline in the down-flow direction. This leaf is very important when the vehicle has passed the chemical source location. This cloverleaf pattern is selected as it yields significant search in all directions relative to the last detection point and it is achievable within the vehicle maneuvering constraints.

The logic flow diagram in Fig. 8 describes the implementation of the Reacquire-Plume behavior. This behavior will stay active until either chemical is detected or the AUV completes the cloverleaf trajectory N_re times. If chemical is detected, the Maintain-Plume behavior will activate and inhibit the Reacquire-Plume behavior. If N_re repetitions are completed without a chemical detection, then this behavior deactivates, which causes Find-Plume to become the active behavior. While Reacquire-Plume is active the function Cloverleaf is used to issue the heading commands required for the vehicle to follow the cloverleaf-shaped trajectory.

The only free parameters in the design of this behavior are N_re and d_{leaf}. The cloverleaf pattern is repeated to decrease the probability that the vehicle passes through the gaps in the plume and reverts to the Find-Plume behavior when it is near the source. The tradeoff is that the AUV could spend too much search time near the location of a spurious detection. In our experiments, N_re is 3 and d_{leaf} is between 10 and 15 meters.

D. Declare-Source Behavior

There is no clear analog to the AUV Declare-Source behavior for male moths. The male moth does not maneuver in the vicinity of the female moth based on scent alone and then return home to broadcast her location. Instead, while the moth plume tracing relies primarily on sensed pheromone, the final determination as to the location of the female moth could be based on data from multiple sensors, which may include vision, tactile, or even auditory cues. However, for CPT using AUVs, the present state of technology requires that we determine the chemical source location based only on the locations of chemical detection events. Fortunately, we can design AUV maneuvers to increase the accuracy of the declared source location. Therefore, the methodology of the Declare-Source behavior is more engineering-oriented than biologically-inspired. We designed the source declaration logic based on analysis, Monte Carlo simulation, and results of initial field experiments.

Definition: The objective of the Declare-Source behavior is to estimate and declare the chemical source location. The declaration must be accurate and reliable in the sense that it makes no false declarations. This behavior contains a perceptional module for estimating the source location, and an action module for first moving to the source location after it has been estimated and then driving the vehicle to the *home* location.

Due to the design of the maintain and reacquire behaviors, as verified in Monte Carlo simulation and in-water studies, when the AUV is far from the source, the locations at which the AUV loses contact with the plume will be widely separated along the axis of the plume. When the AUV traces the plume to the source location, it will exit the plume and move up flow from the source. In this case, the vehicle activates the Reacquire-Plume behavior. The AUV will usually recontact the plume on Leaf 3 of the clover leaf trajectory since leaves 1 and 2 are upflow from the last detection point. No matter which leaf generates the next detection, the Maintain-Plume behaviors will activate and this sequence of behaviors will repeat. We maintain a list of the last detection points recorded

in the Maintain-Plume behavior. When far from the source, these points are separated along the axis of the plume. When near the source, since the source location is fixed, the 'last detection points' list will accumulate a set of points near but downflow from chemical source location. This list of last detection points is monitored and a suitably close clustering of the furthest upflow points generates the source declaration.

Generally, pushing more last-detection points onto the list, results in more information about the source location being available to the algorithm. Increasing the number of points used in the decision may increase the accuracy and reliability, but may also increase the time required to satisfy the declaration criteria. The final version of the source location estimation module used the M=6 most recent points[1], (x_{last_1}, y_{last_1}), (x_{last_2}, y_{last_2}), …, (x_{last_M}, y_{last_M}). The box for estimating the source location is determined by the three most up-flow of these six points. The sorting with respect to flow direction uses the flow direction vector at the time of the sort. After sorting the list of 6 points in the order of upflow location (i.e., most upflow first), the AMP calculated

$$x_{min} = \min\{x_{last\_1}, x_{last\_2}, x_{last\_3}\}$$
$$x_{max} = \max\{x_{last\_1}, x_{last\_2}, x_{last\_3}\}$$
$$y_{min} = \min\{y_{last\_1}, y_{last\_2}, y_{last\_3}\}$$
$$y_{max} = \max\{y_{last\_1}, y_{last\_2}, y_{last\_3}\}.$$

When the diameter of box satisfies

$$R = \sqrt{(x_{max} - x_{min})^2 + (y_{max} - y_{min})^2} \leq \varepsilon,$$

the source location is estimated as

$$x_{source} = 0.5(x_{min} + x_{max})$$
$$y_{source} = 0.5(y_{min} + y_{max}).$$

The value for ε is affected mainly by the vehicle dynamics and the accuracy of the navigation system. The REMUS AUV had a turning radius estimated between 5 and 10 m depending on vehicle speed and the navigation systems was expected to typically be accurate to better than 10 m. For our experiments ε was 3m to 5m.

The Declare-Source behavior includes a Go-To-Goal module for driving the AUV to the source location and then driving the AUV home. The Go-To-Goal module issues heading commands $\theta = \text{atan2}((y_{target} - y), (x_{target} - x))$ that will direct the vehicle from its current location to a target location. The target location is the declared source location until the AUV is within 10 m of that location. Then the target location is switched to the predefined *home* location.

The Declare-Source activity is continually monitoring the list of last-detection points, but its output is inactive until the declaration condition is satisfied. After that time, since it is the highest priority behavior, the outputs of the Declare-Source behavior determine the AUV trajectory.

V. IN-WATER RESULTS

The AMP strategy described herein was tested in November 2002 at San Clemente Island on a REMUS vehicle. The REMUS has been developed by the Oceanographic Systems Laboratory at the Woods Hole Oceanographic Institute. The REMUS vehicle is designed to be small, lightweight, and highly accurate in terms of navigational performance and sensor data. The maximum operation depth is 100 m, and the velocity range is from 0.25 m to 2.8 m/s. The testbed REMUS vehicle contained two PC-104 computers. The first computer system (REMUS) implemented the standard REMUS propulsion, control, navigation, and sensor processing algorithms. The second computer system (AMP) implemented the CPT strategy. The AMP sends guidance (i.e. heading, speed, and altitude) commands to the REMUS via a serial port. The AMP is responsible for interrupting the pre-programmed REMUS mission (i.e. Mission A in Fig. 1), performing its plume tracing task (i.e. Mission B in Fig. 1), and then returning the REMUS to its preprogrammed mission.

The REMUS vehicle is equipped with a variety of sensors, including a fluorometer, side-scan sonar, and conductivity, temperature, and depth sensors. The REMUS also carries sensors to provide information about the current operating state of the vehicle, including the vehicle latitude and longitude, depth and altitude, heading and speed, and water flow velocity. The REMUS implements control and guidance functions with which the AMP will interact.

The AMP implements safety logic that prevents the four plume tracing behaviors from driving the REMUS significantly outside of the OpArea. When one of the behaviors causes REMUS to reach a boundary, the behavior is overridden by a safety behavior that returns REMUS to the OpArea. If at any time the REMUS location is greater than 30 m outside of the OpArea, the AMP will relinquish control and REMUS will resume the preprogrammed task of Mission A.

The values of the CPT algorithm parameters that were used in the experiments are summarized in Table 1. The parameters were selected prior to the in-water tests and not tuned during the experiments unless specifically stated in the following. The parameters in Table 1 are based on the results described [19] and additional simulation studies that included realistic AUV, flow, and plume models. The chemical plume for these tests was Rhodamine dye[2]. The dye was pumped from the source at a controlled rate as listed in Table 2.

This set of tests included 17 vehicle runs. We describe the runs in two batches. The first 10 tens ended unsuccessfully for various reasons: MSN001 – aborted due to an OpArea data entry problem; MSN001r2 – abort after starting plume tracing due to an incorrect timeout setting; MSN002 – aborted due to start-up problems; MSN003 – traced and declared but for chemical that was not the actual plume for this run; MSN004

---

[1] It is natural to ask why the value M=6 was selected. In the first ten runs, we used M=3 without successful source declaration. Based on analysis of that mission data, we saw that the last detection points often alternated between being near the source and being further downstream. To have three points on the list that were near the source therefore required M=6. To have the three most upflow be first on the list, the list had to be sorted with respect to flow direction.

[2] Color images of the source with the plume and AUV are available on the first and second authors' web sites, but are not included herein as they do not render well on black and white printed media.

– CPT performed well, but source declaration never occurred; MSN005 – aborted due to equipment failure; MSN006 – CPT performed well, but source declaration never occurred; MSN007r1 – CPT performed well on chemical that was not the actual plume for this run. MSN003 and MSN007r1 are anomalous runs due to dye previously in the water flowing back through the OpArea. This set of runs used a list of the most recent M=3 points to define the source declaration rectangle and ε = 3 m in the source declaration logic. In MSN004 and MSN006 CPT functioned well, but source declaration did not occur. Based on analysis of the data from MSN004 and MSN006, in the source declaration logic we changed to M=6, ε = 4 m, and sorted the list based on upflow location as described in Section IV-D. Of these changes, increasing the value of M and sorting the list based on upflow location were the most important. In the previous logic, using only the three most recent points resulted in a source estimation rectangle that was long in the direction of the flow. The remainder of the analysis in this section will only be concerned with the next seven runs which are labeled as MSN007r2 — MSN010r3.

For the last seven runs, the OpArea, source location, flow conditions, and chemical pump rate are summarized in Table 2. For missions MSN007r2—MSN009, the OpArea was defined by a box with corners: NW (130, -46) m, SW (55, -129) m, SE (-130, 46) m, NE (-55, 129) m. This box is approximately 254 m by 112 m. The long axis is rotated by 47 deg west of north. For missions MSN010r1—MSN010r3, the OpArea was defined by a box with corners: NW (148, -63) m, SW (72, -146) m, SE (-148, 63) m, NE (-72, 146) m. This box is approximately 300 m by 112 m. The long axis is also rotated by 47 deg west of north and is approximately parallel to the shoreline. The fourth column of Table 2 also lists the AMP range of ocean flow speed and direction as computed onboard REMUS by AMP. For example, for missions MSN007r2, the flow speed and direction are in the range of [0.08, 0.12] m/s and [124°, 146°], respectively. The temporal variation in the computed flow is shown in Fig. 9(a)-(b).

Trajectory and chemical detection data for three runs are shown in Figs. 10, 11 and 12. In each of these figures, the curve with circles at each end is the vehicle trajectory. Each 'x' along the trajectory indicates the location of a chemical detection. The rectangle indicates the boundary of the OpArea. One circle indicates the REMUS position at the start of Mission B. The other circle indicates the declared source location. Note that the actual REMUS location is a continuous function of time; however, the computed REMUS location may change discontinuously as the result of navigation corrections generated after receiving signal from an in-water transponder network. Such navigation corrections are evident near the coordinates (-75, 25) in Fig. 11 and (10, 20) in Figure 12. Numerous smaller corrections also occur during the runs. Such navigation corrections complicate the task of source declaration.

For these experiments, the source was affixed to the ocean bottom and could not move. Therefore, the start of the plume as indicated by the most upflow detection locations should be fixed relative to the bottom. However, comparison of Figs. 10, 11, and 12 shows that the apparent plume starting point to

be different in each of these the runs. The difference for Figs. 10 and 11 relative to Fig. 12 is easily explained, since the OpArea definition was enlarged and shifted after MSN009. The difference between Figs. 10 and 11 is due the setup of the navigation system that is affected by operational issues, ocean flow, and tide conditions. The (N,E) position is computed using transponders in the water column that are tethered to the ocean floor. If the transponder locations change, then the entire coordinate system is shifted accordingly. For example, when the batteries in the transponders require replacement, the transponder-tether-anchor system is pulled up and then reinserted at its nominal location. Reinsertion involved divers getting a differential GPS reading at the surface near the location at which the transponder equipment was lowered approximately 20 meters on a cable. DGPS inaccuracy plus sway introduced by water motion between the boat on the surface relative to the anchor at the bottom of the cable may introduce error. Also the flow and tides affect the position of the transponder buoys which shifts the coordinate system relative to the ocean floor. Note that the nominal source location is computed via GPS and is unaffected by flow conditions. Therefore, the nominal source and declared source location listed in Table 3 should not be used as the only methods of performance analysis. Post-mission plots such as those in Figs. 10, 11, and 12 are further evidence that the source declarations were accurate based on the chemical detection data. For Fig. 12, it should be noted that the REMUS was not allowed to venture more than 30 meters outside the OpArea and that detections outside the OpArea were ignored by the CPT algorithm; therefore, the declared location is based on the most upflow detection data available to the AMP. Finally, for this set of experiments, a video camera was in the water and focused on the chemical source. The camera captured many images of the AUV operating near the source just prior to its returning to the home location, which provides yet another means to verify tracing of the chemical plume to its source.

Table 3 records data related to start location, source declaration location, and the time cost of the vehicle maneuvers. All stated locations are in the (N, E) coordinate frame. The second column lists the starting location on one line with the declared-source location underneath. The third column indicates the error between the declared source location and the nominal source location. Among the various runs, the vehicle starting location was varied, with the objective of forcing different experimental conditions. For example, as shown in Fig. 11, the start position for MSN008r1 was located at (49, -97) m, and the vehicle started by using the down-flow Plume-Finding behavior. As shown in Fig. 12, the start position for MSN010r2 was located at (–60, 71) m, but the flow direction was now to the northwest; therefore, the vehicle started at the opposite end of the search area, but again used the down-flow Plume-Finding behavior. Note that it required several seconds for the AUV to change from its initial upflow heading to the commanded downflow search direction. In each of these last 7 runs, the Find-Plume, Maintain-Plume, and Reacquire-Plume behaviors were impressive and in each case the source declaration logic succeeded.

The accuracies of the declared locations relative to the nominal source locations, as recorded in Table 3, are on the order of tens of meters. Given that the vehicle navigation sys-

tem accuracy is also approximately 10 m and that the area covered by this level of uncertainty is small relative to the size of the search area, this level of performance was quite satisfactory. Even so, these accuracies must be interpreted with caution. In addition to the possible errors between the coordinate systems of the nominal source and the declared source locations the following factor could affect the accuracy of the reported locations. Due to the fact that the chemical source is on the bottom and the vehicle is driving at a nonzero altitude, the chemical will not be detected in the immediate vicinity of the source. The chemical will only be detected at a distance in the down-flow direction that is sufficient for the chemical plume to rise to the altitude of the vehicle. Therefore, the declared source location is known to be some distance down-flow from the source. This down-flow direction is known, but the distance is not known since the distance depends on environmental factors. Therefore, the likely source location is within a long narrow rectangle. The long edge is parallel to the flow. The down-flow narrow edge is centered on the declared source location. Calibration of the errors between the transponder relative declared source location and earth fixed nominal source location will be a major issue addressed prior to subsequent in-water testing.

To analyze the efficiency of the CPT strategy, we define the following times: t_0 is the time at which Mission B starts; t_1 is the first time that chemical is detected; t_2 is the first time that the plume is traced to within 13 m of the declared source location for that run; and, t_3 is the time at which the source location is declared. Note that the time t_2 is not known during the mission and can only be computed via post-processing. The time spent searching for the plume is $T_f = t_1 - t_0$. The time spent tracking the plume from the first detection point to a point within 13 meters of the declared location is $T_T = t_2 - t_1$. Time t_2 will be referred to as the time at which the source was found – even though the AMP did not actually declare until time t_3. After first approach within 13 m of the declared source, the time spent maneuvering prior to declaring the source location is $T_D = t_3 - t_2$. The total CPT mission time is $T_{Total} = T_f + T_T + T_D$. Columns 4 — 7 of Table 3 provide this data as well as the corresponding percentage times for each of the last seven AMP test runs. Usually, the REMUS vehicle follows the search cycle: plume-found, source-found, source-declared. Except for MSN007r2, each run started with the AMP algorithm using the Find-Plume behavior. During MSN009 and MSN010r1, the vehicle activated the Find-Plume behavior twice, because in the first search cycle the REMUS failed to declare the source location even though it found the source location. For those two runs, two values of t_1, t_2, and t_3 are presented. The first value of t_3 is the time at which the AMP switched back to the Find-Plume behavior due to the failure in the source declaration.

The longest time to find the plume was 905.4 seconds in the second search circle of MSN010r1. During the source-finding period $[t_1,t_2]$, the Maintain-Plume and Require-Plume alternatively activate to steer the REMUS toward to the odor source location. The longest time interval to find the source is 228.0 seconds in MSN007r2, but its time cost just was 32.1% of the total time cost for that test run. During the source-declared period $[t_2, t_3]$, the Maintain-Plume and Reacquire-Plume behaviors kept the REMUS near the odor source loca-

tion. The test data show that in each case the revised Declare-Source algorithm declared the odor source location correctly; however, typically the source declaration time T_D was significantly more than three times the tracking time T_T. The longest time interval for the source-declared maneuver is 550.4 seconds during MSN008r1. The largest source-declared percentage was 91.3% in the test run MSN008r2.

Table 4 presents data to allow analysis of the search efficiency in terms of distance traveled. D_0 is the Euclidean distance between the position at which chemical is first detected at time t_1 and the source location declared at t_3 :

$$D_0 = \sqrt{(x_{t_3} - x_{t_1})^2 + (y_{t_3} - y_{t_1})^2} \ .$$

D_0 may be defined as the ideal minimum path for plume tracing. D_0 is not expected to be achievable due to maneuverability issues, and meander and intermittency of the real plume; however, it provides a useful benchmark. D_1 is the actual travel distance during the time interval $[t_1, t_2]$ which is computed as

$$D_1 = \sum \sqrt{(x_{t+1} - x_t)^2 + (y_{t+1} - y_t)^2}, t \in [t_1, t_2] \ .$$

D_1 is the distance traveled to track the plume to within 13 m of the declared source location for the first time. D_2 is the distance traveled during the time interval $[t_2, t_3]$ which is computed as

$$D_2 = \sum \sqrt{(x_{t+1} - x_t)^2 + (y_{t+1} - y_t)^2}, t \in [t_2, t_3] \ .$$

D_2 represents the distance traveled between the time the REMUS first gets within 10 m of the declared source and the time that the source is declared. Finally, the total distance traveled is: $D_3 = D_1 + D_2$.

Except in MSN008r2 and the first search cycle of MSN009, the actual travel distance for plume tracing D_1 is larger than the ideal plume length D_0. The largest ratio of D_1 to D_0 is 3.9 in the first search cycle of MSN010r1. The average ratio of D_1 to D_0 is 1.3 which is considered quite good as the average amount that D_1 could be decreased is only 23%. The biggest D_0 is 164.2m in MSN007r2 where D_1 is 411.0m. We do not include the ratio of D_2 to the other distances, because D_2 is not expected to scale with the length of the plume. From the data, it is clear that the majority of each mission was spent in the process of making the source declaration. This allows significant room for improvement; however, care must be taken to ensure that improved speed of declaration does not sacrifice the reliability of the declaration in the sense that this algorithm made no false declarations.

VI. CONCLUSIONS

This article has presented an AMP strategy for finding and tracing a chemical plume and declaring a source location using a subsumption architecture. The strategy was implemented on a REMUS vehicle and tested in near shore ocean conditions. For these experiments, the OpArea was 250-300 m along shore and 100 m cross-shore. Plumes were tracked for over 100 m. At the time of these experiments, this AMP strategy was the first reported instance of chemical plume tracing in a "real world" environment, the search area was the largest in which chemical plume tracing experiments were

attempted, the experiments were the first to successfully and reliably declare a source location, and the results demonstrated the longest instances of chemical plume tracking.

The source declaration accuracy can only be characterized as accurate to tens of meters, due to issues related to the nominal source location being in a distinct coordinate system and parameters for the proper transformation between the coordinate systems being unknown and time varying. This issue has motivated two changes to be implemented prior to future in-water testing. First, after source declaration the AMP will implement a fly-by maneuver to drive the AUV past the declared source location in the downflow direction. Since there is a camera focused on the source, this maneuver will allow visual confirmation of correct declared source locations. Second, after source declaration, the AMP will implement a maneuver to acquire sidescan sonar data in the vicinity of the declared location. Since sidescan data are calibrated within the same coordinate system as the source declaration, this approach will allow absolute comparisons between the declared and actual source locations.

The purpose of the in-water experiments was demonstration and evaluation of the CPT approach and acquisition of chemical distribution data along a plume in a near shore ocean environment. Evaluation of alternative algorithms or of algorithm performance as a function of algorithm parameters would have been interesting, but was precluded by the time and cost of running the in-water tests. However, we have analyzed the efficiency of the present algorithm. The Find-Plume, Maintain-Plume, and Reacquire-Plume behaviors were robust and worked well. By robust, we mean that the algorithms succeeded many times under different experimental conditions without any changes to the parameters of the algorithms. On the other hand, while the present source declaration approach was successful in the sense that it never made an invalid declaration, due to the difficulty of the source declaration problem based on olfaction alone, the time and distance travel to make the declarations leaves significant room for improvement in the future.

Finally, a last important lesson learned in this experiment is that the altitude control algorithm achieves an altitude above the commanded altitude when the water depth is increasing (offshore direction) and an altitude below the commanded altitude when the water depth is decreasing (onshore direction). Therefore, because the REMUS was at a lower altitude when driving toward from shore and because the plume is near the bottom, the REMUS was more likely to detect chemical when driving toward shore.

REFERENCES

[1] D. B. Dusenbery, Sensory Ecology: How Organisms Acquire and Respond to Information, New York: W. H. Freeman, pp. 385-405, 1992.

[2] N. J. Vickers, "Mechanisms of animal navigation in chemical plumes," *Biological Bulletin*, vol. 198, pp. 203-212, 2000.

[3] R. K. Zimmer and C. A. Butman, "Chemical signaling processes in the marine environment," *Biological Bulletin*, vol. 198, pp. 168-187, 2000.

[4] A. D. Hassler and A. T. Scholz, *Olfactory Imprinting and Homing in Salmon*, Springer-Verlag, New York, pp. 13-40, 1983.

[5] G. A. Nevitt, "Olfactory Foraging by Antarctic Proellariiform Seabirds: Life at High Reynolds Numbers," *Biological Bulletin*, vol. 198, pp. 245-253, 2000.

[6] J. Basil and J. Atema, "Lobster orientation in turbulent chemical plumes: simultaneous measurements of tracking behavior and temporal chemical patterns," *Biological Bulletin*, vol. 187, pp. 272-273, 1994.

[7] D. V. Devine and J. Atema, "Function of Chemoreceptor organs in spatial orientation of the lobster, Homarus americanus: Differences and overlap," *Biological Bulletin*, vol. 163, pp. 144-153, 1982.

[8] M. J. Weissburg and R. K. Zimmer-Faust, "Chemical plumes and how blue crabs use them in finding prey," *J. Exp. Biol.*, vol. 197, pp. 349-375, 1994.

[9] R. T. Cardé, *Odour plumes and odour-mediated flight in insects. In Olfaction in Mosquito-Host Interactions*, CIBA Found. Symp, 200: John Wiley & Sons, pp. 54-70, 1996.

[10] R. T. Cardé and A. Mafra-Neto, "Mechanisms of flight of male moths to pheromone." In R.T. Cardé and A.K. Minks (eds.), *Insect Pheromone Research. New Directions*, Chapman and Hall, New York, pp. 275-290, 1996.

[11] J. S. Elkinton, C. Schal, T. Ono, and R. T. Cardé, "Pheromone puff trajectory and upwind flight of male gypsy moths in a forest," *Physiological Entomology*, vol. 12, pp. 399-406, 1987.

[12] P. Rau and N. L. Rau, "The sex attraction and rhythmic periodicity in the giant saturniid moths," *Transactions of the Academy of Science of Saint Louis,* vol. 26, pp. 82–221, 1929.

[13] J. A. Farrell, S. Pang, and W. Li, "Plume mapping via Hidden Markov methods," *IEEE Trans on Systems, Man, and Cybernetics-Part B: Cybernetics,* vol. 33, pp. 850-863, 2003.

[14] F. W. Grasso, T. Consi, D. Mountain, and J. Atema, "Locating chemical sources in turbulence with a lobster inspired robot," *From Animals to Animats 4: Proceedings of the Fourth International Conference on Simulation of Adaptive Behavior* (P. Maes, M. J. Mataric, J.-A. Meyer, J. Pollack, and S. W. Wilson, Eds), MIT Press, pp. 104-112, 1996.

[15] J. H. Belanger and M. A. Willis, "Adaptive control of chemical -guided location: Behavioral flexibility as an antidote to environmental unpredictability," *Adaptive Behavior*, vol. 4, pp. 217-253, 1998.

[16] J. H. Belanger and M. A. Willis, "Biologically-inspired search algorithms for locating unseen odor sources," *Proceedings of the IEEE International Symposium on Intelligent Control*, pp. 265-270, 1998.

[17] F. W. Grasso, T. R. Consi, D. C. Mountain, and J. Atema, "Biomimetic robot lobster performs chemo-orientation in turbulence using a pair of spatially separated sensors: Progress and challenges," *Robotics and Autonomous Systems*, vol.30, pp. 115-131, 2000.

[18] F. W. Grasso, "Invertebrate-Inspired Sensory-Motor Systems and Autonomous, Olfactory-Guided Exploration," *Biological Bulletin*, vol.200, pp. 160-168, 2001.

[19] W. Li, J. A. Farrell, and R. T. Cardé, "Tracking of fluid-advected chemical plumes: Strategies inspired by insect orientation to pheromone," *Adaptive Behavior*, vol. 9, pp. 143-170, 2001.

[20] R. A. Russell, D. Thiel, R. Deveza, and A. Mackay-Sim, "A robotic system to locate hazardous chemical leaks," *Proceedings of 1995 IEEE Inter. Conf. on Robotics and Automation,"* vol. 1, pp. 556–561, 1995.

[21] H. Ishida, Y. Kagawa, T. Nakamoto, and T. Moriizumi, "Chemical-source localization in the clean room by an autonomous mobile sensing system," *Sensors and Actuators B*, vol. 33, pp. 115-121, 1996.

[22] H. Ishida, T. Nakamoto, T. Moriizumi, T. Kikas, and J. Janata, "Plume-tracking robots: A new application of chemical sensors," *Biological Bulletin*, vol.200, pp. 222-226, 2001.

[23] Y. Kuwana, S. Nagasawa, I. Shimoyama, and R. Kanzaki, "Synthesis of the pheromone-oriented behavior of silkworm moths by a mobile robot with moth antennae as pheromone sensors," *Biosensors & Bioelectronics*, vol.14, pp. 195-202, 1999.

[24] F. W. Grasso and J. Atema, "Integration of flow and chemical sensing for guidance of autonomous marine robots in turbulent flows," *Journal of Environmental Fluid Mechanics*, vol. 1, pp. 1-20, 2002.

[25] S. Kazadi, R. Goodman, D. Tsikata, and H. Lin, "An autonomous water vapor plume tracking robot using passive pesistive polymer sensors," *Autonomous Robots*, 9(2), pp. 175-188, 2000.

[26] L. Marques, U. Nunes, and A. T. de Almeida, "Olfaction-based mobile robot navigation," *Thin Solid Films*, vol. 418, p. 51-58, 2002.

[27] A. T. Hayes, et al., "Distributed chemical source localization," IEEE Sensors Journal, vol. 2, pp. 260-271, 2002.

[28] R. M Arrieta, J. A. Farrell, W. Li, and S. Pang, "Initial development and testing of an adaptive mission planner for a small unmanned underwater vehicle," *Proc. of OMAE03 22nd International Conference on Offshore Mechanics and Arctic Engineering*, OMAE2003-37273, 2003.

[29] J. A. Farrell, W. Li, S. Pang, and R. M Arrieta, "Chemical plume tracing experimental results with a REMUS AUV," *Proc. of Ocean 2003 Marine Technology and Ocean Science Conference,* pp. 962-978, 2003.

[30] J. Murlis, "The structure of odour plumes," In T. L. Payne, M. C. Birch, and C. E. J. Kennedy (eds.), *Mechanisms in insect olfaction,* pp. 27-38, 1986.

[31] C. D. Jones, "On the structure of instantaneous plumes in the atmosphere," *Journal of Hazardous Materials*, vol. 7, pp. 87-112, 1983.

[32] D. R. Webster and M. J. Weissburg, "Chemosensory guidance cues in a turbulent chemical odor plume," *Limnology Oceanography*, 46(5), pp. 1034-1047, 2001.

[33] C. M. Finelli, N. D. Pentcheff, R. K Zimmer-Faust, and D. S. Wethey, "Odor transport in turbulent flows: constraints on animal navigation," *Limnology Oceanography*, 44(4), pp. 1056-1071, 1999.

[34] E. Yee, D. J. Wilson, and B. W. Zelt, "Probability distributions of concentration fluctuations of a weakly diffusive passive plume in a turbulent boundary layer," Boundary-Layer Meteorology, 64(4), pp. 321-354, 1993.

[35] J. A. Farrell, J. Murlis, W. Li, and R. T. Cardé, "Filament-Based Atmospheric Dispersion Model to Achieve Short Time-Scale Structure of Chemical Plumes", *Environmental Fluid Mechanic*s, vol. 2, pp. 143-169, 2002.

[36] H. Schlicting and K. Gersten, *Boundary-layer theory,* 8th Edition, Springer-Verlag, New York, pp. 29-48, 2000.

[37] M. T. Stacey, E. A. Cowen, T. M. Powell, E. Dobbins, S. G. Monismith, and J. R. Koseff, "Plume dispersion in a stratified, near-coastal flow: measurements and modeling," *Continental Shelf Research*, vol. 20, pp. 637-663, 2000.

[38] M. A. Willis, J. Murlis, and R. T. Carde, "Pheromone-mediated upwind flight of male gypsy moths, *Lymantria dispar*, in a forest," *Physiological Entomology*, Vol. 16, pp. 507-521, 1991.

[39] M. Arbib, *Perceptional Structures and Distributed Motor Control, Handbook of Physiology* – The Nervous System, Vol. II, Motor Control, Part 1 (V.B. Brooks, Ed.), American Physiological Society, pp. 1449-1480, 1981.

[40] V. Braitenberg, *Vehicles: Experiments in Synthetic Psychology*, MIT Press, Chapters 1-5, 1984.

[41] R. A. Brooks, "A robust layered control system for a mobile robot," *IEEE J. Robot. Automation RA-2***,** pp. 14-23, 1986.

[42] R. C. Arkin and R. R. Murphy, "Autonomous navigation in a manufacturing environment," *IEEE Trans. Robot. Automation RA-6*, pp. 445-454, 1990.

[43] W. Li, "Fuzzy-logic-based reactive behavior control of an autonomous mobile system in unknown environments," *Engineering Application of Artificial Intelligence*, vol. 7, no. 5, pp. 521-531, 1994.

[44] A. Saffiotti, E. H. Ruspini, and K. Konolige, "Blending reactivity and goal-directness in a fuzzy controller," *Proc. of the IEEE International Conference on Fuzzy Systems,* pp. 134-139, 1993.

[45] W. Li, C. Y. Ma, and F. M.Wahl, "A neuro-fuzzy system architecture for behavior-based control of a mobile robot in unknown environments," *Fuzzy Sets and Systems*, vol. 87, pp. 133-140, 1997.

[46] M. W. Sabelis and P. Schippers, "Variable wind directions and anemotactic strategies of searching for an odour plume," *Oecologia*, vol. 63, pp. 225-228, 1984.

[47] D. B. Dusenbery, "Optimal search direction for an animal flying or swimming in a wind or current," *Journal of Chemical Ecology*, vol.15, pp. 2511-2519, 1989.

[48] M. J. Weissburg, "The Fluid Dynamical Context of Chemosensory Mediated Behavior," *Biological Bulletin*, vol. 198, pp. 188-202, 2000.

[49] D. R. Webster, S. Rahman, and L. P. Dasi, "On the Usefulness of Bilateral Comparison of Tracking Turbulent Chemical Odor Plumes," *Limnol. Oceanogr.*, Vol. 46, pp. 1048-1053, 2001.

[50] L. P. S. Kuenen and R. T. Cardé, "Strategies for recontacting a lost pheromone plume: Casting and upwind flight in the male gypsy moth," *Physiological Entomology,* vol.19, pp. 15–29, 1994.

[51] J. S. Elkinton and R. T. Cardé, "Appetitive flight behavior of male gypsy moths (Lepidoptera: Lymantriidae)," *Environmental Entomology*, vol.12, pp. 1702–1707, 1983.

[52] J. Murlis, J. S. Elkinton, and R. T. Cardé, "Chemical plumes and how insects use them," *Annual Review of Entomology*, vol. 37, pp. 505-532, 1992.

Wei Li (M' 94) received B.S. (1982) and M.S. (1984) degrees in electrical engineering from the Northern Jiaotong University, Beijing, P.R. China, and a Ph.D. (1991) in electrical and computer engineering from the University of Saarland, Germany. He was a faculty member of Computer Science and Technology, at Tsinghua University (1993-2001). From 1999 to 2001, he was a Research Scientist of the Department of Electrical Engineering at the University of California, Riverside. Currently he is a Professor with the Department of Computer Science at California State University, Bakersfield.

Dr. Li received the 1995 National Award for Outstanding Postdoctoral Researcher in China and the 1996 Award for Outstanding Young Researcher at Tsinghua University. He was a Croucher Foundation Research Fellow (1996) at City University of Hong Kong and an Alexander von Humboldt Foundation Research Fellow at the Technical University of Braunschweig, Germany (1997-1998). His research interests are intelligent systems, robotics, fuzzy logic control and neural networks, multisensor fusion and integration, and graphical simulation.

Jay A. Farrell (M'86–SM'97) received B.S. degrees (1986) in physics and electrical engineering from Iowa State University, and M.S. (1988) and Ph.D. (1989) degrees in electrical engineering from the University of Notre Dame. At Charles Stark Draper Lab (1989-1994), he was principal investigator on projects involving intelligent and learning control systems for autonomous vehicles. Dr. Farrell received the Engineering Vice President's Best Technical Publication Award in 1990, and Recognition Awards for Outstanding Performance and Achievement in 1991 and 1993. He is a Professor and former Chair of the Department of Electrical Engineering at the University of California, Riverside. His research interests include: identification and on-line control for nonlinear systems, integrated GPS/INS navigation, and artificial intelligence techniques for autonomous vehicles. He is co-author of the books "Adaptive Approximation Based Control" (Wiley 2005) and "The Global Positioning System and Inertial Navigation" (McGraw-Hill, 1998) and over 120 additional technical publications.

Shuo Pang (M'06) received the B.Eng. degree (1997) in electrical engineering from Harbin Engineering University, China and the M.S. (2001) and Ph.D. (2004) degrees in electrical engineering from University of California, Riverside. Currently he is an Assistant Professor in the Department of Computer and Software Engineering at Embry-Riddle Aeronautical University, Daytona Beach, FL. Dr. Pang's current research interests include: embedded control systems, robotics, and autonomous vehicles, e.g. AUV and UAV.

Richard M. Arrieta received his B.S. (1988) in mechanical engineering from Caltech and M.S. (1989) in mechanical engineering from Stanford University. He is Head of the U.S. Navy SPAWAR Systems Center –San Diego's Ocean Technology Branch and Project Manager for their Unmanned Maritime Vehicle (UMV) Laboratory. His team supports fleet Unmanned Underwater Vehicle (UUV) activities, the Office of Naval Research, Explosive Ordnance Disposal Program Office, and Department of Defense on the subject matter of unmanned vehicles and sensors for mine countermeasures, shallow water surveys, anti-terrorism, force protection, and Intelligence, Surveillance, Reconnaissance missions.
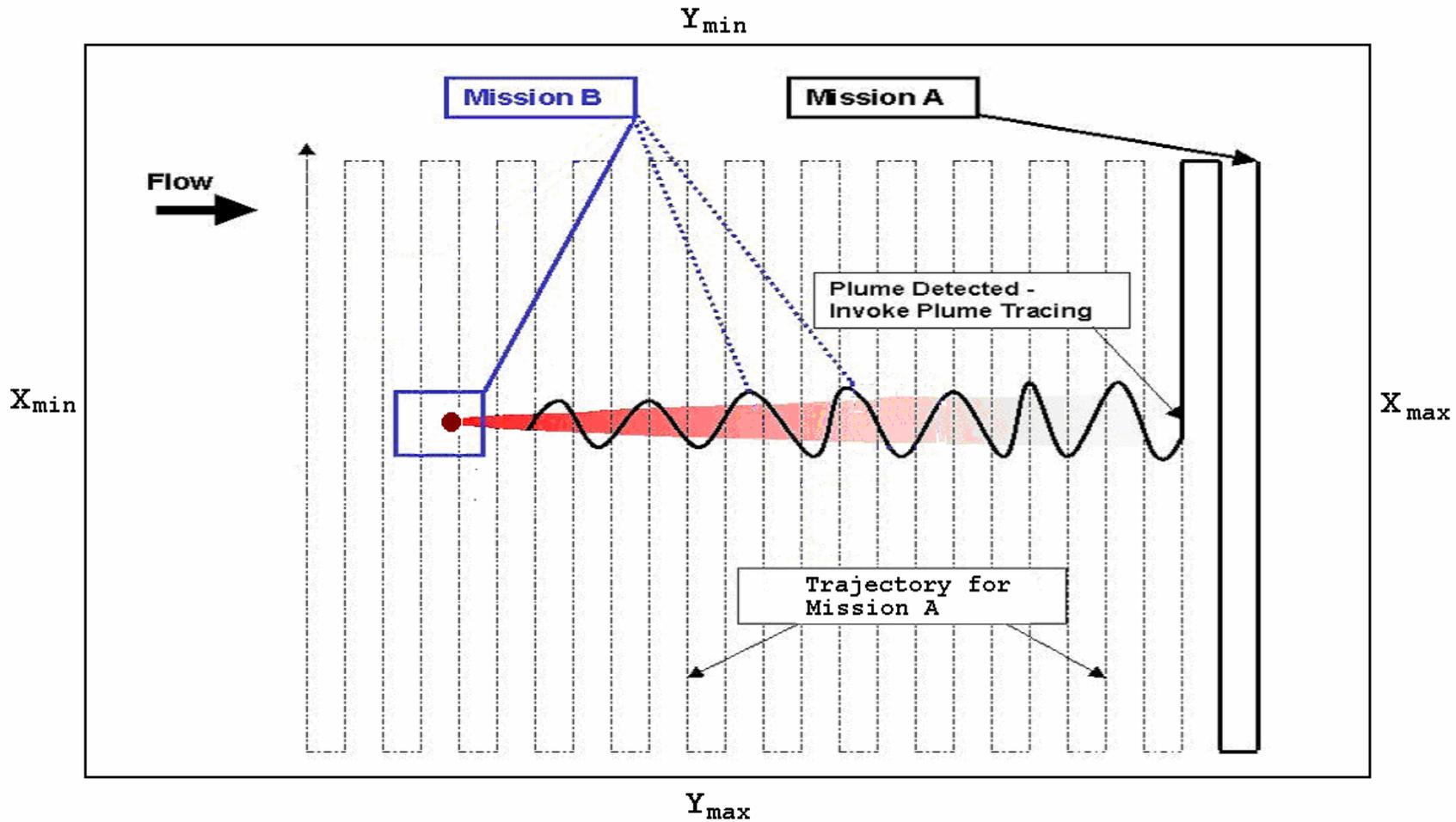
Fig. 1: Ideal plume tracing in the planning coordinate system. The solid black line indicates the actual AUV trajectory including preplanned (Mission A) and reactively planned (Mission B) portions. The circle indicates the chemical source. The flow is drawn positive to the right. The shaded cone emanating from the source depicts a highly simplified chemical plume.
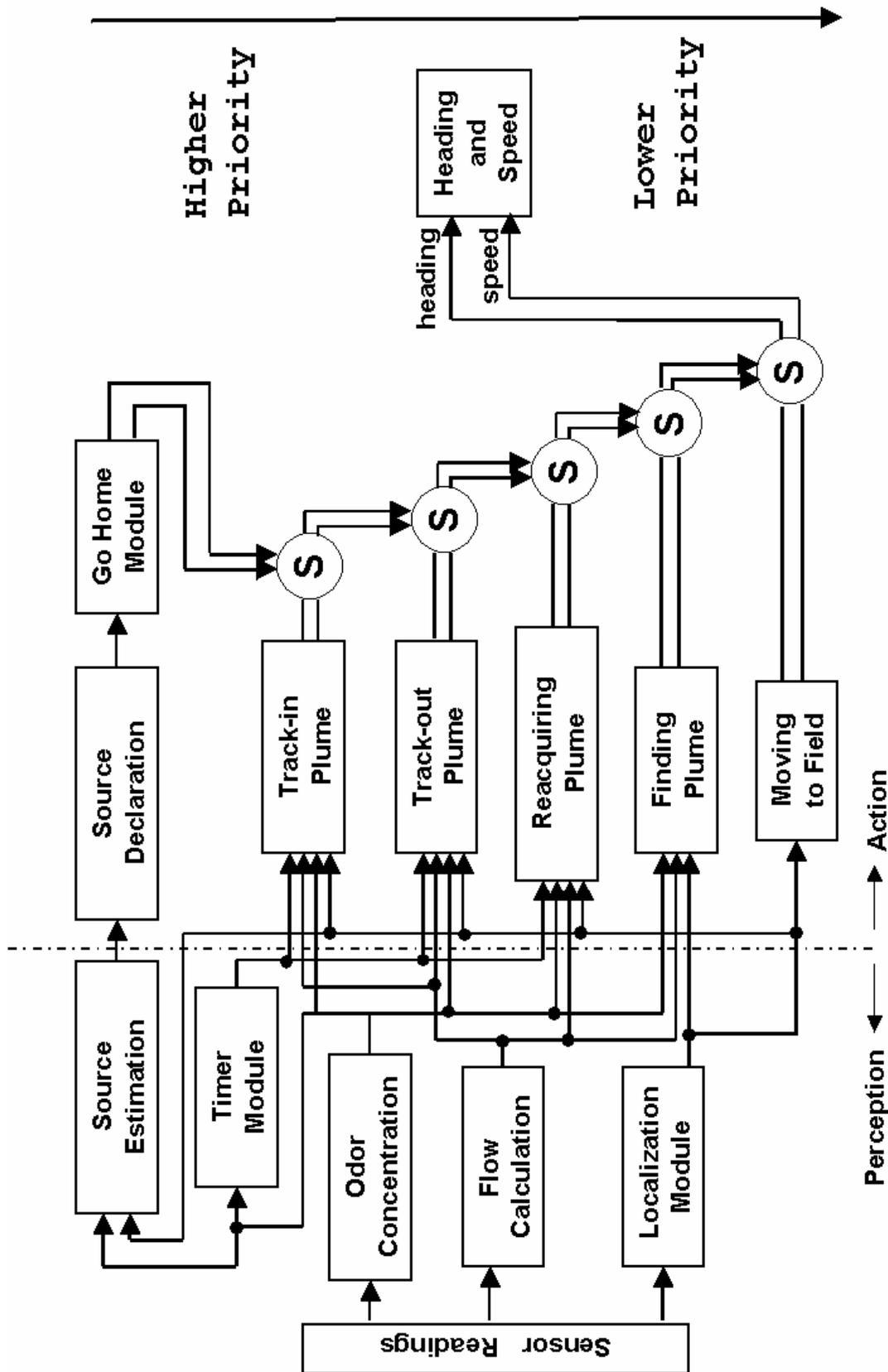
Fig. 2. Subsumption architecture for the Chemical Plume Tracing Adaptive Mission Planner.
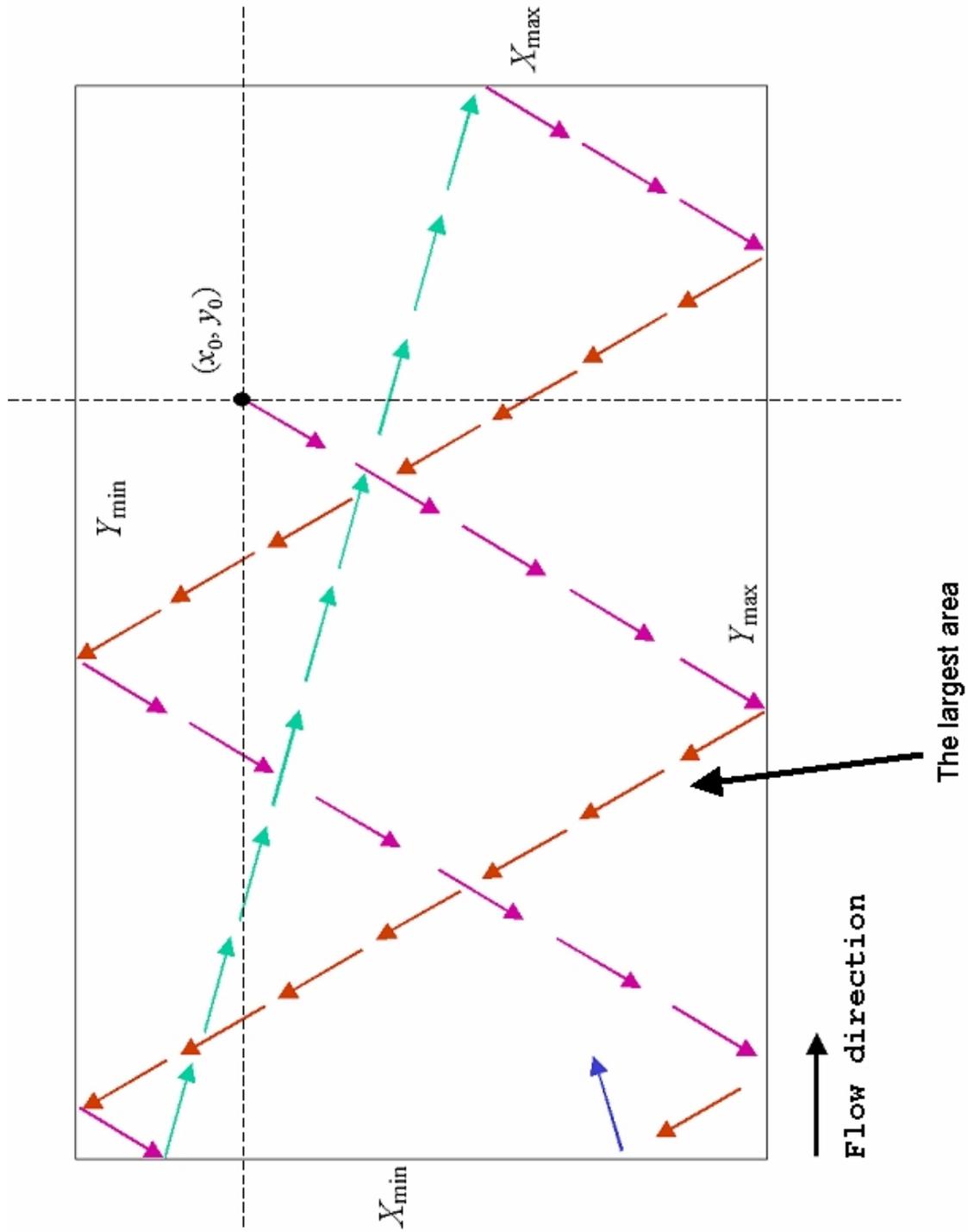
Fig. 3: An idealized trajectory for the Find-Plume behavior.

14
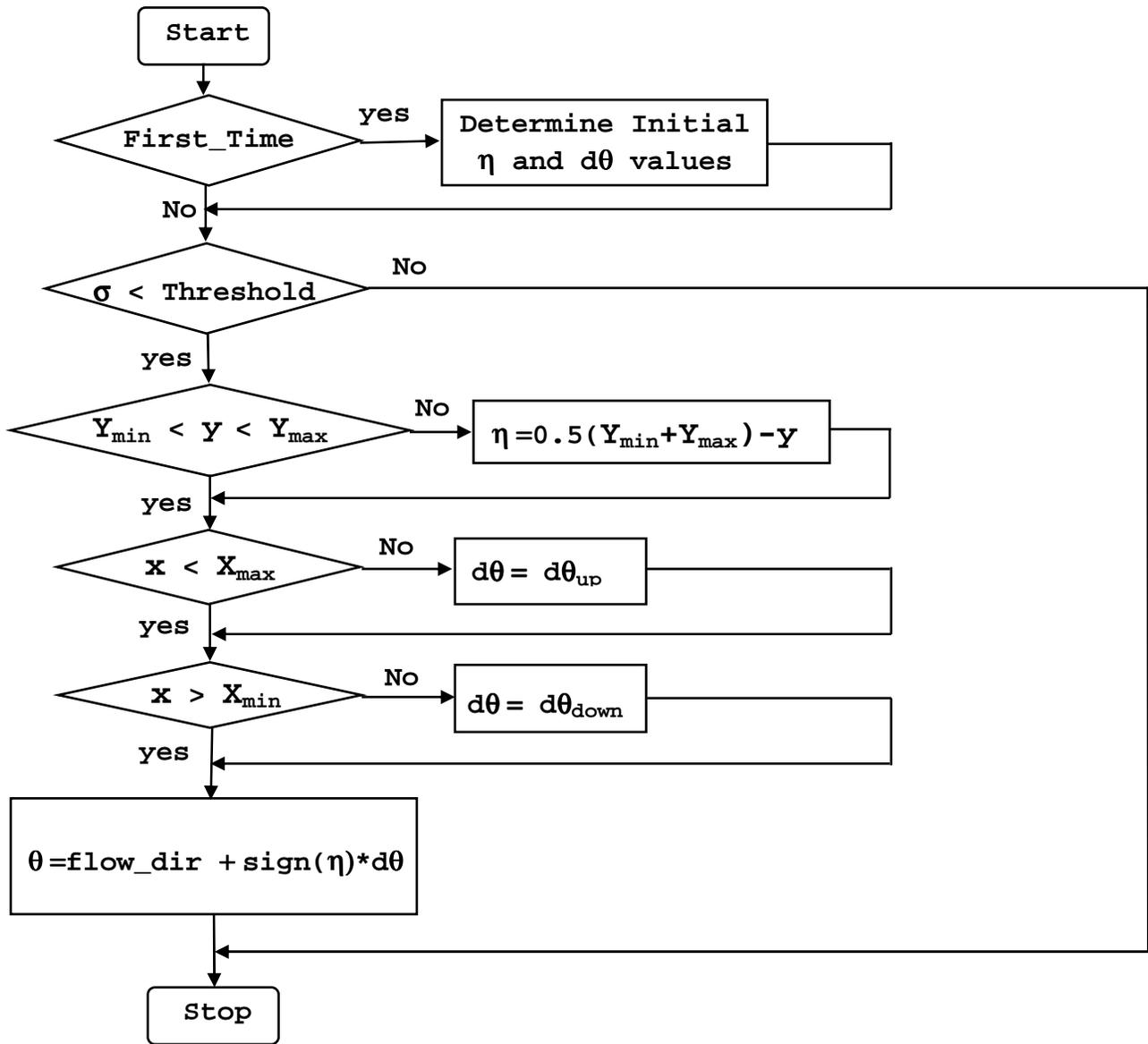
Fig. 4. Logic Diagram for the Find-Plume behavior. The current vehicle location in planning coordinates is (x,y). The planning space OpArea is a rectangle aligned with the axes with lower left corner at (Xmin,Ymax) and upper right corner at (Xmax,Ymin). The sense chemical concentration is σ. The commanded heading and speed are θ and ν.
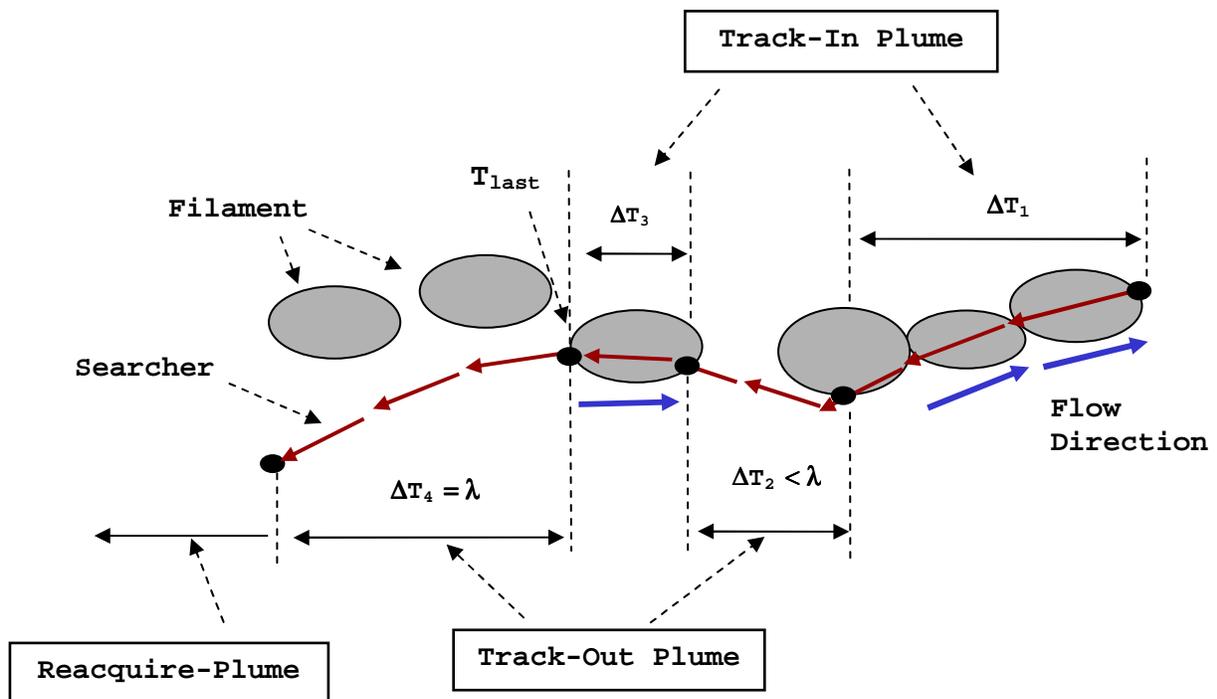
Fig. 5. Track-In and Track-Out actions in the Maintain-Plume behavior.

```
                    ┌──────────┐
                    │  Start   │
                    └──────────┘
                         │
                         ▼                         No
              ◇ σ > Threshold ◇ ──────────────────────────┐
                         │                                  │
                   Yes   │                                  ▼
                         │                          ◇ (t - T_last)<=λ ◇ ── No ──┐
                         ▼                                  │                    │
              ┌────────────────────┐                  Yes  │                    │
              │ θ = flow_dir + 180° │                       ▼                    │
              │ T_last = t          │        ┌──────────────────────────────┐   │
              │ x_last = x          │        │ θ = flow_dir + 180°+β(t)     │   │
              │ Y_last = y          │        └──────────────────────────────┘   │
              └────────────────────┘                       │                    │
                         │ ◄──────────────────────────────┘                    │
                         │ ◄──────────────────────────────────────────────────┘
                         ▼
                    ┌──────────┐
                    │   Stop   │
                    └──────────┘
```
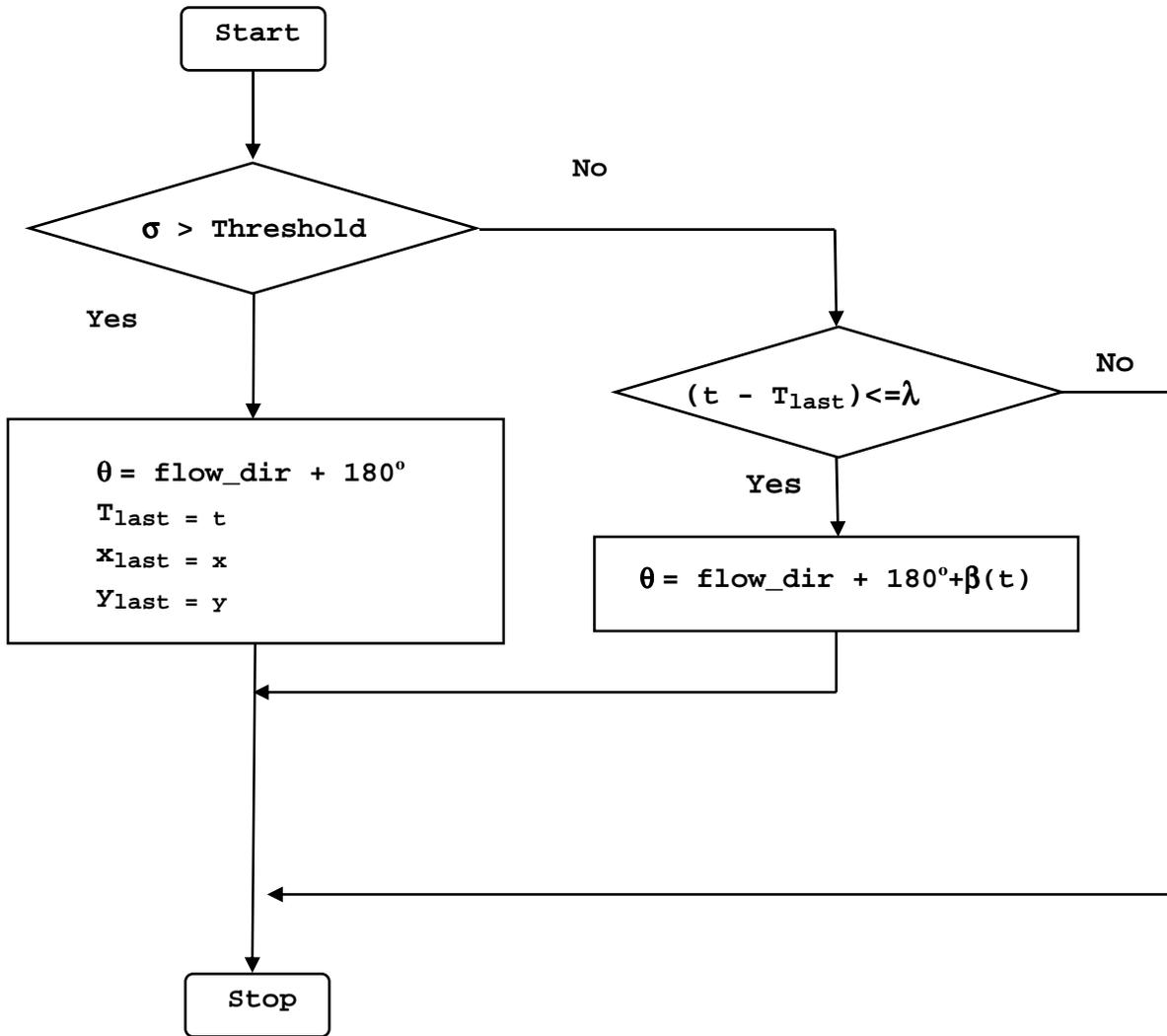
Fig. 6. Logic diagram for the Maintain-Plume behavior. The Track-In action is defined by the left path. The Track-Out action is defined by the right two paths. The variables (x_{last}, y_{last}) are saved for possible later use by the Reacquire-Plume behavior.

17
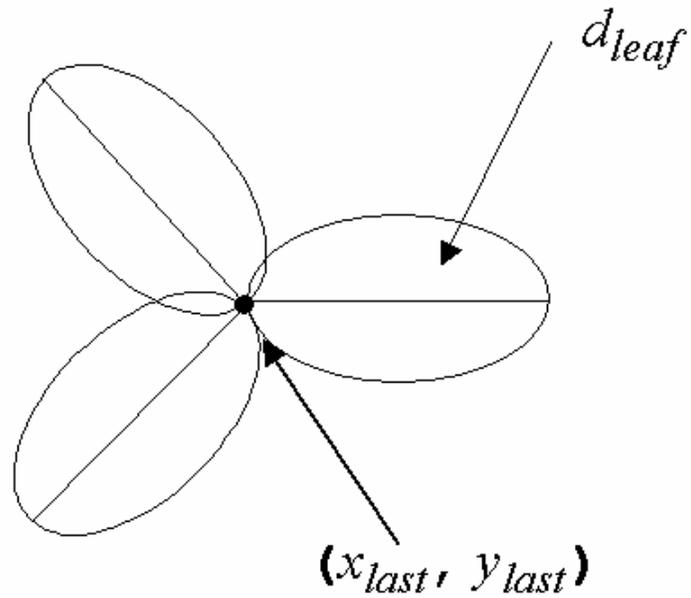
Fig. 7. The clover leaf trajectory for the Reacquire-Plume behavior. The orientation of the trajectory in this figure assumes that the flow is from left to right. The maneuver is centered on the last detection point.

```
                    ┌─────────┐
                    │  Start  │
                    └─────────┘
                         │
                         ▼
           ╱─────────────────╲      Yes      ┌─────────┐
          ◄   First_Time      ►───────────►  │  n = 0  │
           ╲─────────────────╱               └─────────┘
                    │ No
                    ▼
           ╱─────────────────╲      Yes
          ◄   σ > Threshold   ►─────────────────────────►
           ╲─────────────────╱
                    │ No
                    ▼
           ╱─────────────────╲      No
          ◄    n < N_re       ►──────────────────────►
           ╲─────────────────╱
                    │ Yes
                    ▼
       ╱─────────────────────────╲   Yes    ┌─────────┐
      ◄   Cloverleaf(n) == done   ►───────► │  n=n+1  │
       ╲─────────────────────────╱          └─────────┘
                    │ No
                    ▼
       ┌─────────────────────────┐
       │   Execute Cloverleaf(n) │
       └─────────────────────────┘
                    │
                    ▼
              ┌─────────┐
              │  Stop   │
              └─────────┘
```
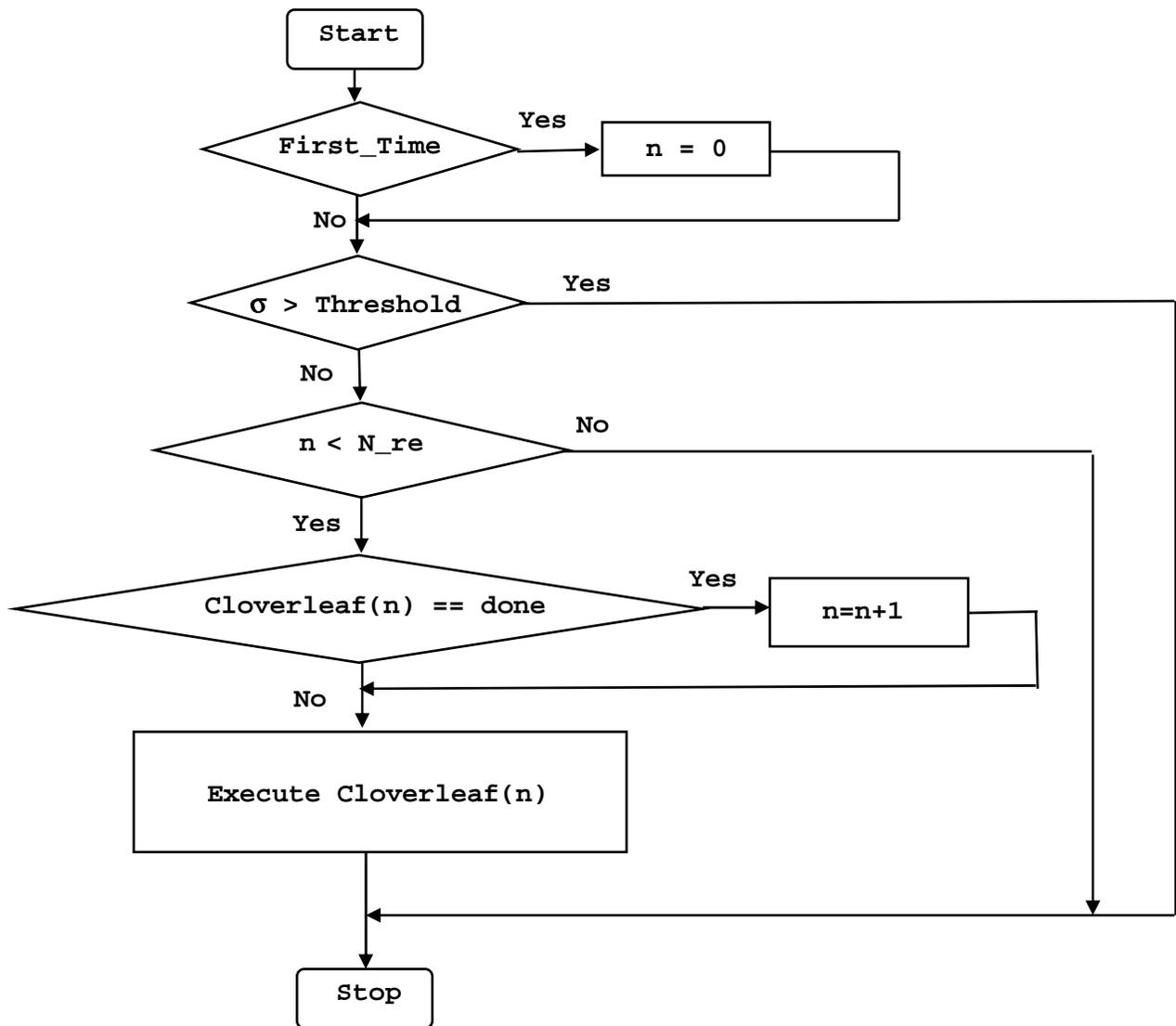
Fig. 8. Diagram for Reacquire-Plume behavior action.
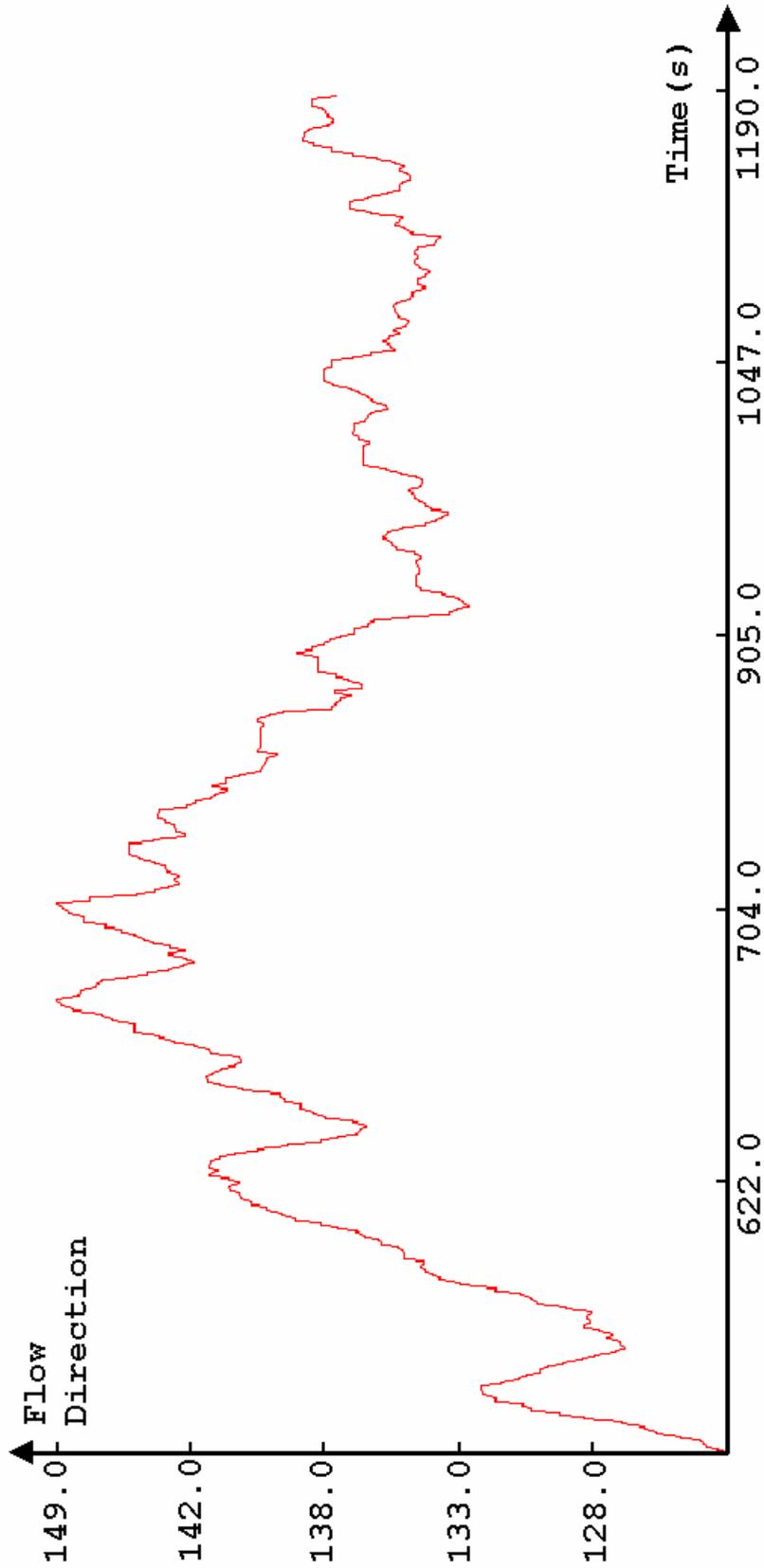
Fig. 9a: Flow direction estimated on the AUV in degrees for t in [480.3, 1190.6] during the mission MSN007r2.
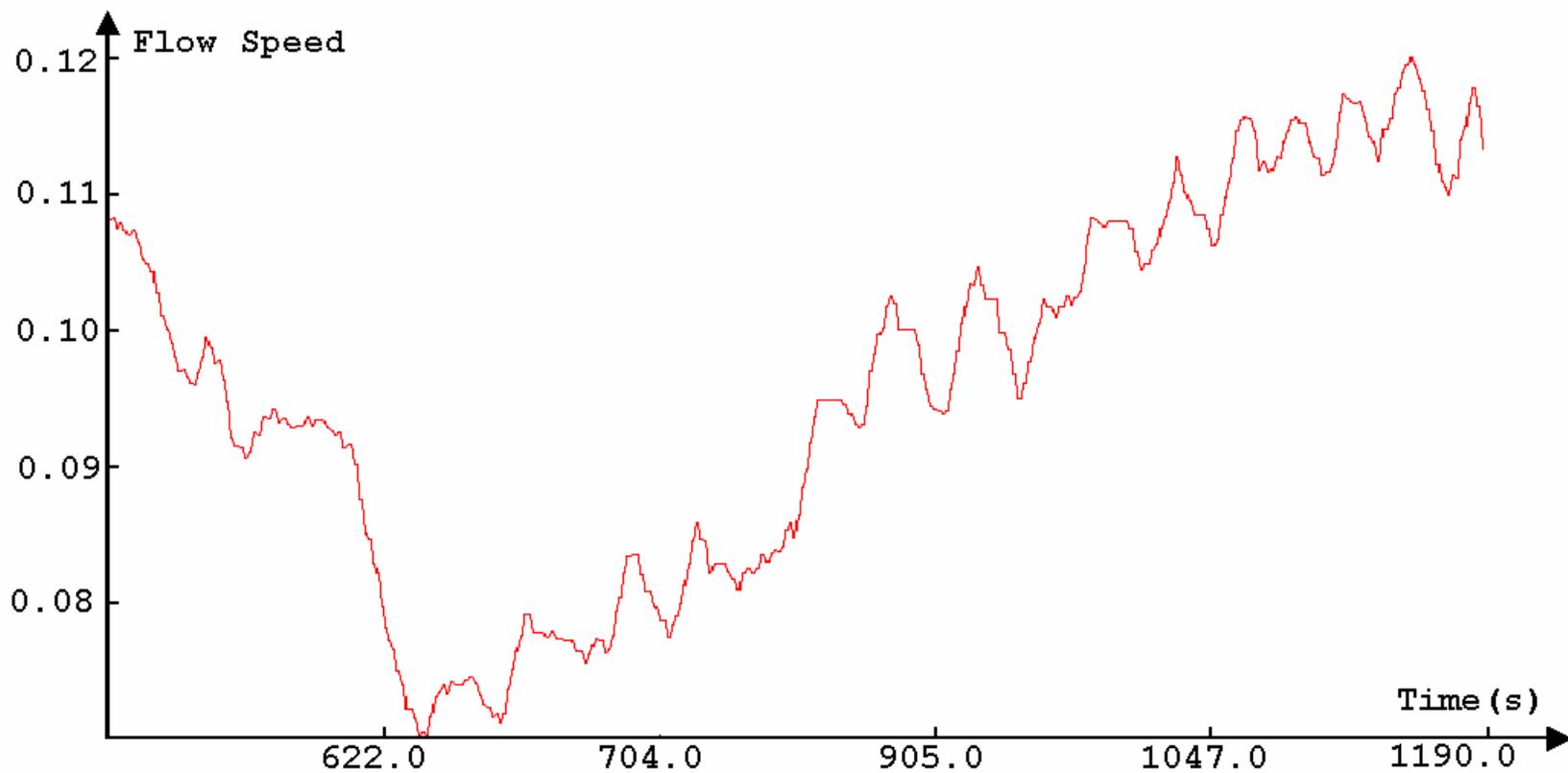
Fig. 9b: Flow speed estimated on the AUV in meters/second for t in [480.3, 1190.6] s during the mission MSN007r2.
Fig. 9. Flow information for chemical plume tracing mission MSN007r2.
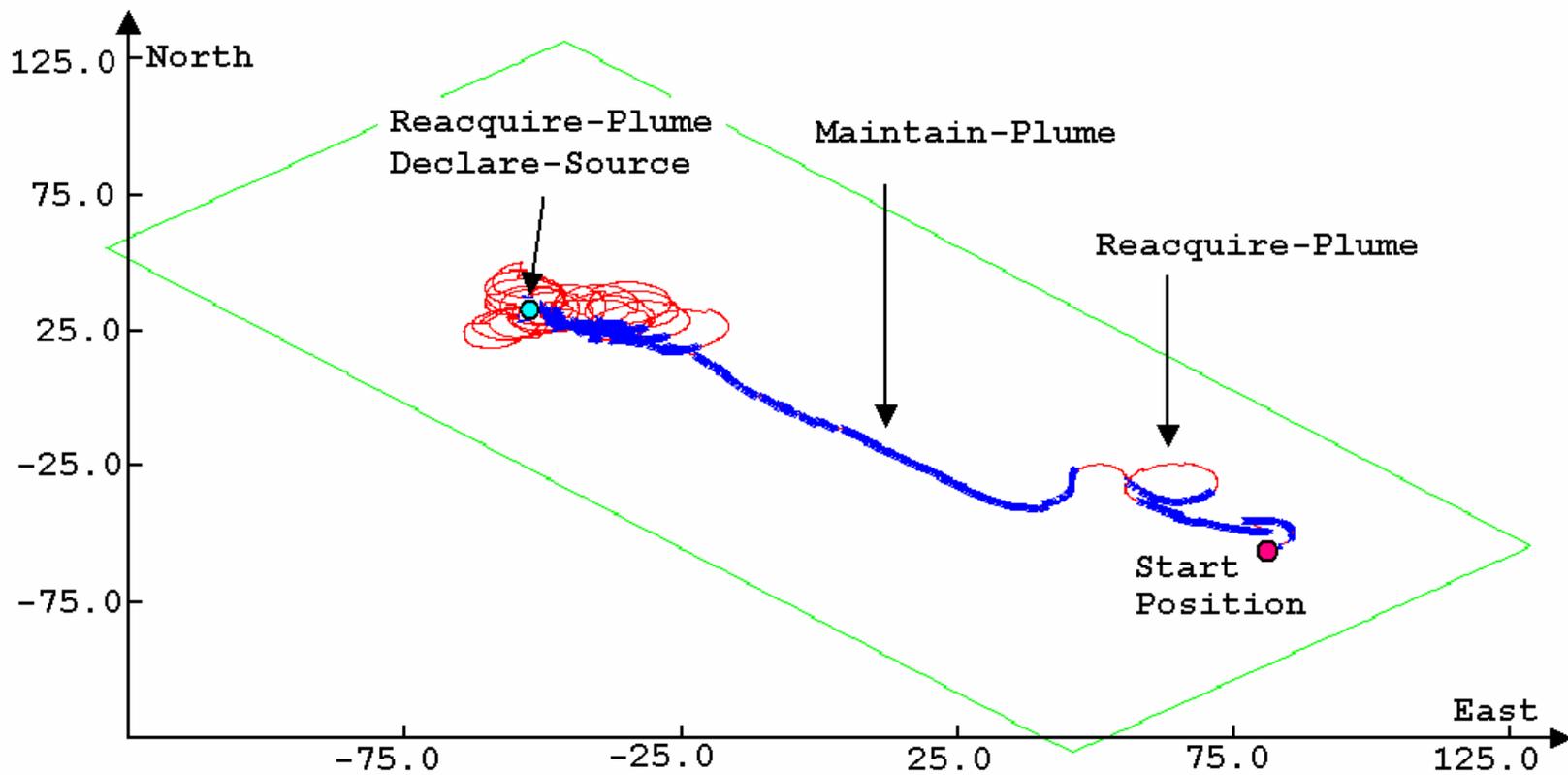
Fig. 10: AUV trajectory during plume tracing and source-declaration for t in [480.3, 1190.6] s during mission MSN007r2. This time period includes Maintain-Plume, Reacquire-Plume, and Declare-Source behaviors. The blue-thick x's indicate locations where the chemical concentration was above threshold when the vehicle was at that location.
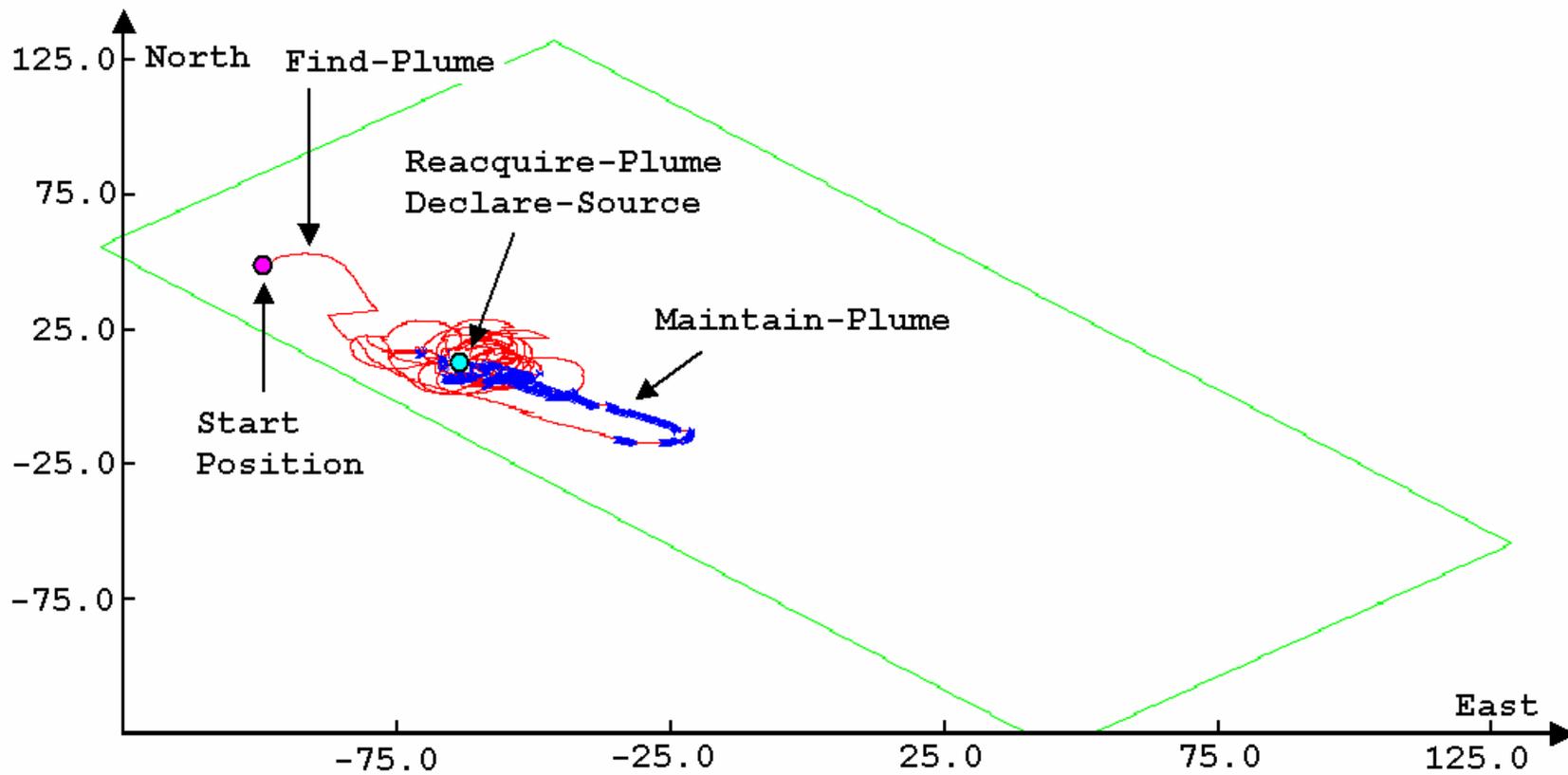
Fig. 11. Chemical plume tracing mission MSN008r1 for t in [60.3, 707.6] s. This time period includes Find-Plume, Maintain-Plume, Reacquire-Plume, and Declare-Source behaviors. The blue-thick x's indicate locations where the chemical concentration was above threshold when the vehicle was at that location.
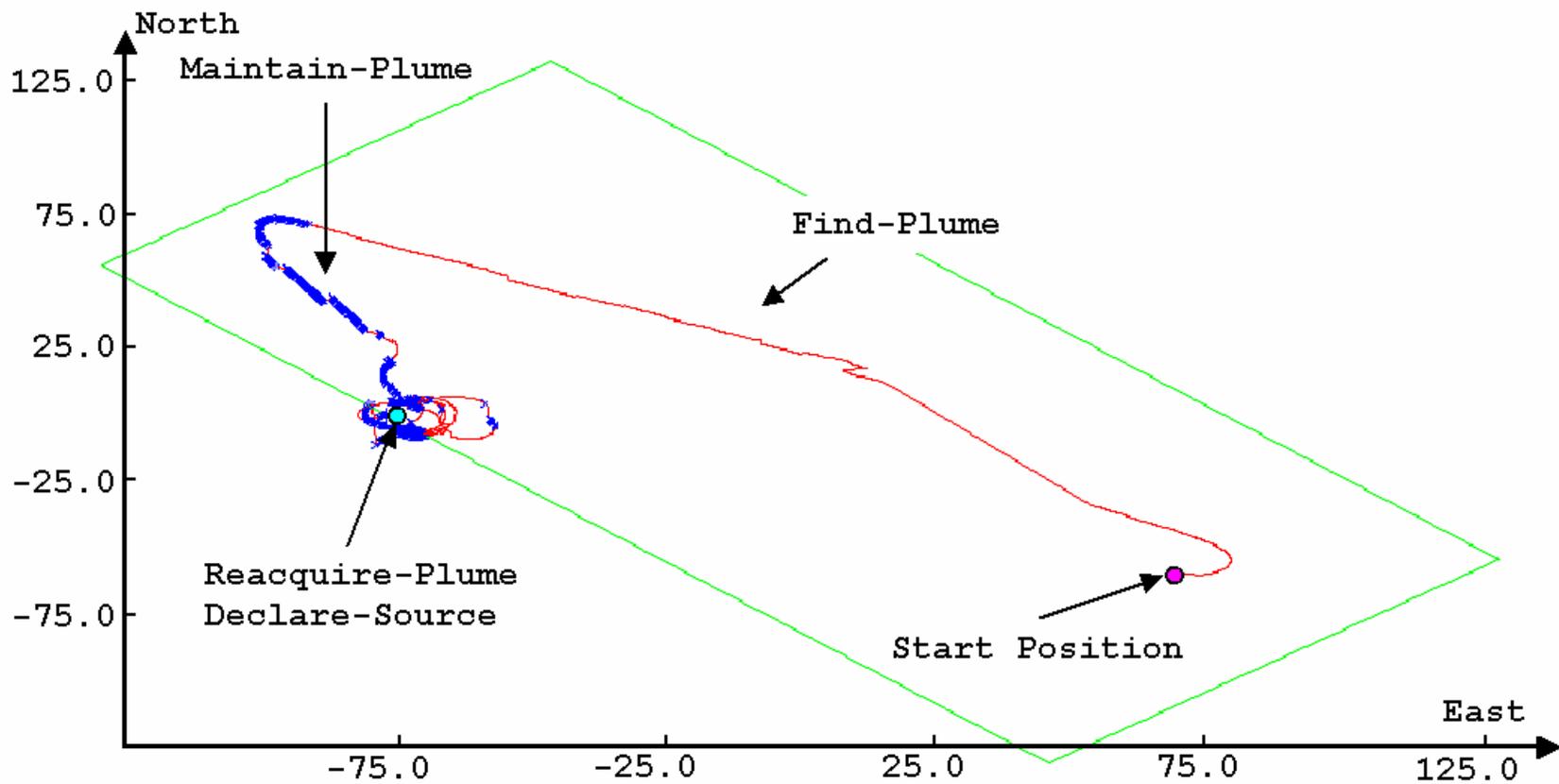
Fig. 12. Chemical plume tracing mission MSN010r2 for t in [80.4, 406.0] s. This time period includes Find-Plume, Maintain-Plume, Reacquire-Plume, and Declare-Source behaviors. The blue-thick x's indicate locations where the chemical concentration was above threshold when the vehicle was at that location.

Table 1: Parameters of Adaptive Mission Planner

Finding	Maintaining	Reacquiring	Declaring
Up-flow search offset $d\theta_{up} = \pm 125\,deg$ Down-flow search offset $d\theta_{down} = \pm 60\,deg$	Waiting time $\lambda = 8.5\,s$ Up-flow motion offset $\beta(t) = \pm 10\,deg$ threshold = 0.20	Diameter of the cloverleaf $d_{leaf} = 15m$ Repetition number N_re = 3	Sorted point number M = 3 (6) Source estimation criterion $\varepsilon = 4\,m$

Table 2: Environment Conditions and Flow information

Run ID	OpArea defined in N-E frame	Nominal Source Location in Geodetic and N-E Frame	Range of Flow Speed and Flow Direction	Chemical Release Rate
MSN007r2		Latitude= 32 n58.867 Longitude=118w32.248	[0.08, 0.12] (m/s) [124°, 146°]	2 gram /min
MSN008r1	The origin (center): Latitude: 32.00 n58.8435 Longitude: 118.00w32.2125	N = 43m E = -55m	[0.05, 0.10] (m/s) [129°, 162°]	2 gram /min
MSN008r2	NW (130, -46) m. SW (54, -129) m. SE (-130, 46) m. NE (-54, 129) m.		[0.02, 0.07](m/s) [122°, 146°]	2 gram /min
MSN009	rotated counter clockwise 47°		[0.03, 0.09] (m/s) [102°, 173°]	1 gram /min
MSN010r1	The origin (center): Latitude = 32.00 n58.853. Longitude=118.00w32.223	Latitude= 32 n58.867 Longitude=118w32.248	[0.02, 0.12] (m/s) [298°, 345°]	1 gram /min
MSN010r2	NW(148, -63) m. SW (72,-146) m. SE (-148, 63) m. NE (-72, 146) m.	N = 26m E = -38m	[0.06, 0.07](m/s) [321°, 353°]	1 gram /min
MSN010r3	rotated counter clockwise 47		[0.03, 0.05] (m/s) [358°, 361°]	1 gram /min

Table 3: Declared-Source Location and Time Cost for Operations

Run ID	Start position and declared-source location in N-E frame, meters	Source declaration error, meters	Time to find plume, seconds T_F , s [t_0 , t_1] T_F / T_{Total}	Time to trace plume, seconds T_T , s [t_1 , t_2] T_T / T_{Total}	Time to declare source, seconds T_D , s [t_2 , t_3] T_D / T_{Total}	Total time, seconds T_{Total} , s [t_0 , t_3]
MSN007r2	(-55.5, 82.9) (28.8, -54.4)	ΔN = -14.6 ΔE = -0.9	0 [480.3, 480.3] 0.0%	228.0 [480.3, 708.3] 32.1%	482.3 [708.3, 1190.6] 67.9%	710.3 [480.3, 1190.6]
MSN008r1	(49.7, -97.8) (6.8, -56.2)	ΔN = -36.6 ΔE = 0.9	67.3 [60.3, 127.6] 10.4%	29.6 [127.6, 157.2] 4.6%	550.4 [157.2, 707.6] 85.0%	647.3 [60.3, 707.6]
MSN008r2	(51.6, -99.2) (14.2, -77.6)	ΔN = -29.2 ΔE = 22.3	26.0 [60.3, 86.3] 8.7%	0.0 [86.3, 86.3] 0.0%	273.4 [86.3, 359.7] 91.3%	299.4 [60.3, 359.7]
MSN009	(-58.0, 33.0) (10.9, -72.3)	ΔN = -32.5 ΔE = -17.7	*500.2* *[60.4, 560.6]* 532.2 [1122.0,1654.2] 69.0%	*0* *[560.6, 560.6]* 28.7 [1654.2, 1682.9] 3.7%	*561.* *[560.6, 1122.0]* 209.6 [1682.9, 1892.5] 27.3%	*1061.6* *[60.4, 1122.0]* 770.5 [1122.0, 1892.5]
MSN010r1	(-56.6, 57.2) (10.0, -85.2)	ΔN = -15.9 ΔE = -47.0	*117.8* *[80.3, 198.1]* *22%* 905.4 [616.5, 1521.9] 75%	*248.9* *[198.1, 447.0]* *46.4%* 0.0 [1521.9, 1521.9] 0.0%	*169.5* *[447.0, 616.5]* *31.6%* 301.0 [1521.9,1822.9] 25.0%	*536.2* *[80.3, 616.5]* 1206.4 [616.5, 1822.9]
MSN010r2	(-60.3, 71.0) (-8.3, -70.4)	ΔN = -33.9 ΔE = -32.2	115.2 [80.4, 195.6] 35.4%	50.3 [195.6, 245.9] 15.5%	160.1 [245.9, 406.0] 49.2%	325.6 [80.4, 406.0]
MSN010r3	(-59.7, 71.0) (-9.6, -44.7)	ΔN = -35.5 ΔE = -6.5	93.1 [80.3, 173.4] 26.1%	15.4 [173.4, 188.8] 4.3%	247.3 [188.8, 436.1] 69.6%	355.8 [80.3, 436.1]

Table 4: Travel Distance for Plume Tracing (Source-Found) and Source-Declared

Run ID	D_0, m	D_1, m	D_2, m	D_3, m	D_1/D_0	D_1/D_3	Source declaration
MSN007r2	164.2	411.0	864.7	1275.7	2.50	32.2%	Yes
MSN008r1	36.7	60.9	1013.1	1074.0	1.66	5.7%	Yes
MSN008r2	9.7	0.0	499.9	499.9	0.0	0.0%	Yes
MSN009	*4.1*	*0.0*	*984.2*	*984.2*	*0.0*	*0.0%*	*No*
	47.0	55.8	371.1	426.9	1.19	13.1%	Yes
MSN010r1	*112.3*	*437.4*	*335.8*	*773.2*	*3.89*	*56.6%*	*No*
	9.2	0.0	568.5	568.5	0.0	0.0%	Yes
MSN010r2	84.2	96.2	293.0	389.2	1.14	24.7%	Yes
MSN010r3	18.8	25.3	435.6	460.9	1.35	5.5%	Yes